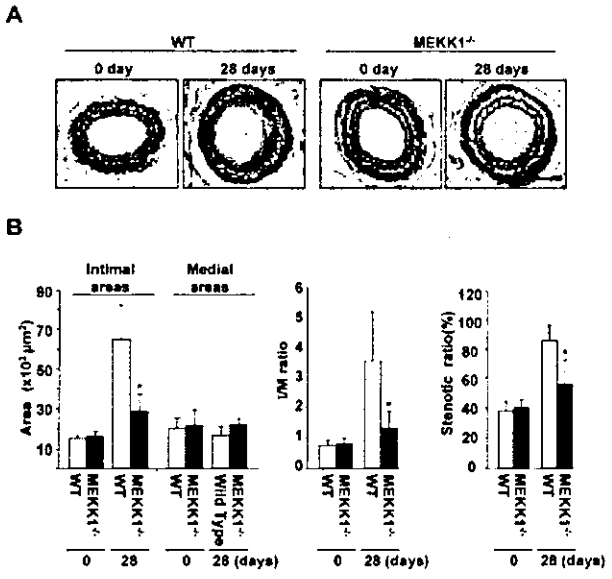

Figure 1. Photomicrographs and morphometry of intimal formation after ligation of carotid arteries. A, Representative cross sections of unligated and ligated carotid arteries on day 28 (elastica van Gieson's stain). Bar indicates 100 μm. B, Quantitative analysis of intimal and medial areas, I-M ratio, and stenotic ratio of ligated arteries. *P<0.05 vs WT mice.

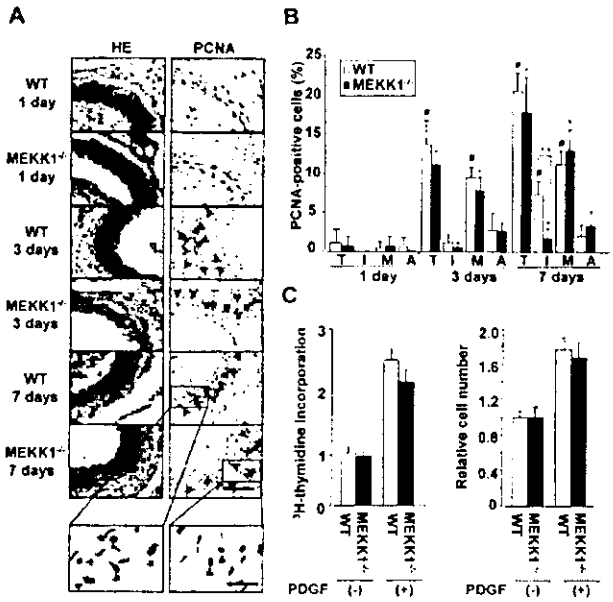

Figure 2. Effects of ablation of MEKK1 on cell proliferation. A, Immunohistochemical analysis of hematoxylin and eosin staining and PCNA staining 1, 3, and 7 days after ligation. Bar indicates 100 μm. Photographs of WT and MEKK1$^{-/-}$ mice 7 days after ligation were enlarged, and bar indicates 30 μm. Red arrowheads indicate PNCA-positive cells. B, Quantification of ratio of PCNA-positive cells to total cell number in arterial wall (T), intima (I), media (M), and adventitia (A) of ligated arteries at 1, 3, and 7 days. Black bars and white bars indicate WT and MEKK1$^{-/-}$ mice, respectively. #P<0.05 vs day 1 in WT mice; *P<0.05 vs day 1 in MEKK1$^{-/-}$ mice; **P<0.05 vs day 7 in WT mice. C, Effects of MEKK1 on PDGF-BB–induced [^{3}H]thymidine incorporation and cell number in AoSMCs. Data are indicated as percentages relative to control group and are mean±SEM of 10 wells in each group of at least 3 replicates.

compared with those 1 day after ligation, but there were no significant differences between WT and MEKK1$^{-/-}$ mice. It is noteworthy that 7 days after ligation, the number of PCNA-positive cells in the intima was significantly less in MEKK1$^{-/-}$ arteries than in WT arteries, although there was no difference within other areas (Figure 2A and 2B). These findings suggest that migration of PCNA-positive cells from the media to the intima was impaired, whereas proliferation was not impaired in MEKK1$^{-/-}$ mice. Consistent with in vivo data, no difference was observed in [^{3}H]thymidine incorporation and cell number between WT and MEKK1$^{-/-}$ AoSMCs after stimulation with PDGF-BB in vitro (Figure 2C). Treatment with EGF or FGF-2 instead of PDGF-BB yielded identical results (data not shown).

Effects of Ablation of MEKK1 on MAPK Activities of AoSMCs

Ablation of MEKK1 does not affect the total protein expression of extracellular signal–regulated kinase (ERK), c-Jun NH_2-terminal kinase (JNK), or p38. We examined the effects of ablation of MEKK1 on MAPK activities of AoSMCs. FGF-2–induced JNK and ERK but not p38 activation in AoSMCs from MEKK1$^{-/-}$ mice was less than that from WT mice (Figure 3A). We confirmed that addition of MEKK1 restored MEKK1 protein levels in MEKK1$^{-/-}$ AoSMCs (Figure 3B). Addition of MEKK1 restored JNK and ERK activation in response to FGF-2 in MEKK1$^{-/-}$ AoSMCs (Figure 3C and 3D). Treatment with EGF or PDGF-BB instead of FGF-2 yielded identical results (data not shown).

MEKK1 Ablation Inhibited AoSMC Migration and Invasion

In the scrape wound–induced migration assays, the average number of and distance that MEKK1$^{-/-}$ AoSMCs migrated from the wound edge (white dotted line) in the absence of any stimulus was similar to those in WT mice; however, the FGF-2–induced increase in cell number and distance was significantly suppressed in MEKK1$^{-/-}$ AoSMCs compared with WT cells. Addition of MEKK1 restored the number and distance of MEKK1$^{-/-}$ AoSMCs to normal levels (Figure 4A and 4B).

In the aortic explant assays, the number of AoSMCs migrating from MEKK1$^{-/-}$ explants at 10 days was considerably lower than those from WT explants (Figure 4C). Moreover, the number of MEKK1$^{-/-}$ aortic explants that showed migrating cells was significantly smaller than in WT explants (27.2±2.2% versus 60.0±2.5%, P<0.05).

In the transwell Matrigel-coated chamber invasion assays, the number of invading MEKK1$^{-/-}$ AoSMCs in response to FGF-2 was suppressed markedly compared with WT cells. Addition of MEKK1 restored the number of MEKK1$^{-/-}$ AoSMCs to normal levels (Figure 4D). Treatment with EGF or PDGF-BB instead of FGF-2 yielded identical results (data not shown).

MEKK1 Ablation Impaired Lamellipodia Formation

There were no morphological differences between WT and MEKK1$^{-/-}$ AoSMCs under basal conditions; however, typi-

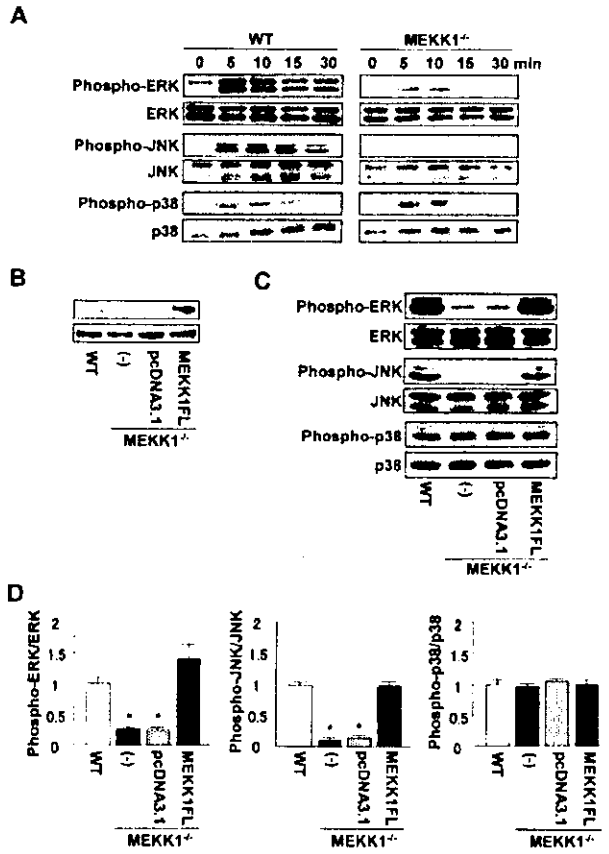

Figure 3. Effects of ablation of MEKK1 on MAPK activities in AoSMCs. A, Time course of JNK, ERK, and p38 activities followed by FGF-2 stimulation. B, Addition of MEKK1 experiments in MEKK1$^{-/-}$ AoSMCs. C, Western blot analysis of MAPKs in MEKK1$^{-/-}$ AoSMCs transfected with empty vector (pcDNA3.1) or full-length forms of MEKK1 vector (MEKK1FL) followed by FGF-2 stimulation. D, Cumulative data for MAPK in Figure 3C. *P<0.05 vs WT AoSMCs.

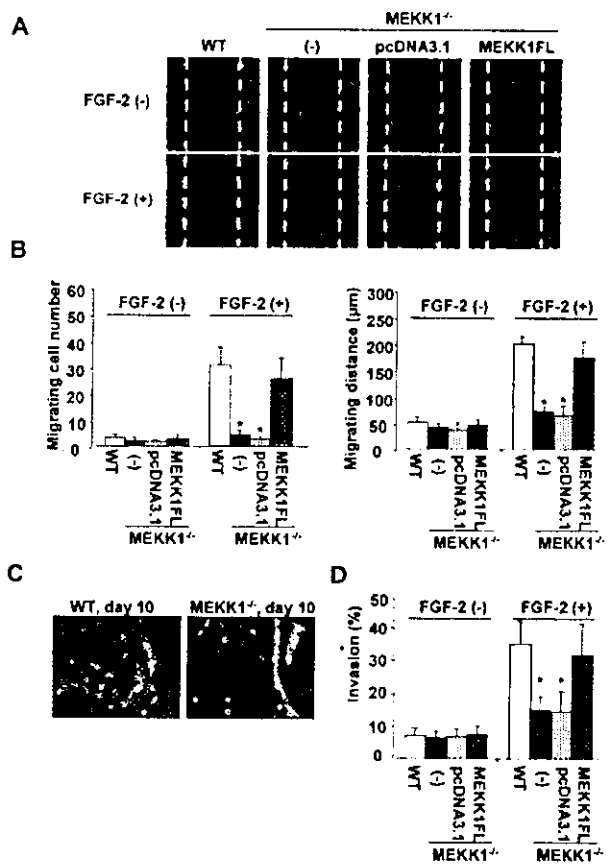

Figure 4. Migration and invasion of AoSMCs. A, Scrape wound–induced migration assay. Immunofluorescence microscopy of migrating cells from wound edge when AoSMCs were cultured for 24 hours with or without FGF-2. F-actin was stained with rhodamine-phalloidin (red), and nuclei were counterstained with DAPI (blue; not visible). B, Quantification of means of number and distance of migrating cells. *P<0.05 vs WT AoSMCs. C, Migration of AoSMCs from aortic explants on day 10. D, Quantification of percent invasion of AoSMCs by transwell Matrigel-coated chamber invasion assay. *P<0.05 vs WT AoSMCs.

cal lamellipodia formation was induced by treatment with EGF in WT AoSMCs but was seldom induced in MEKK1$^{-/-}$ AoSMCs (Figure 5A). The percentage of MEKK1$^{-/-}$ AoSMCs showing lamellipodia was significantly lower than in WT AoSMCs (P<0.05). Addition of MEKK1 restored the lamellipodia-forming capacity of MEKK1$^{-/-}$ AoSMCs (Figure 5B). Treatment with FGF-2 or PDGF-BB instead of EGF yielded identical results (data not shown).

MEKK1 Ablation Decreased uPA Expression

uPA expression began to increase on day 1 and reached a peak on day 3, after which it decreased gradually by 7 days after ligation in WT mice. In contrast, there was only weak positive staining for uPA up to 7 days in MEKK1$^{-/-}$ mice (Figure 6A). In vitro immunofluorescence staining revealed that PDGF-BB–induced uPA expression was decreased in MEKK1$^{-/-}$ AoSMCs compared with those of WT mice (Figure 6B). Western blotting showed a dramatic reduction of FGF-2–induced uPA expression in MEKK1$^{-/-}$ AoSMCs, which was restored by addition of MEKK1 (Figure 6C).

Discussion

Several lines of evidence suggest that MEKK1 is implicated in diverse biological responses.[6–8] Recently, the unique role of MEKK1 in regulating the migration of several cell types has aroused widespread attention[9,12,27] and inspired us to study its involvement in cardiovascular diseases. Up to now, there has been no previous report on the role of MEKK1 in the development of vascular remodeling, during which invasion and proliferation of SMCs play key roles. In the present study, we investigated the mechanism whereby MEKK1 regulates vascular remodeling in a well-established, blood-flow cessation model in MEKK1$^{-/-}$ mice. We found that MEKK1 is essential for intimal hyperplasia after cessation of blood flow.

In this study, we clearly demonstrated that intimal areas, I-M ratios, and stenotic ratios of the ligated arteries were significantly lower in MEKK1$^{-/-}$ mice relative to WT mice, indicating that MEKK1 is implicated in intimal hyperplasia. Although an angioplasty/balloon injury model would have yielded greater applicability to the clinical situation, we used

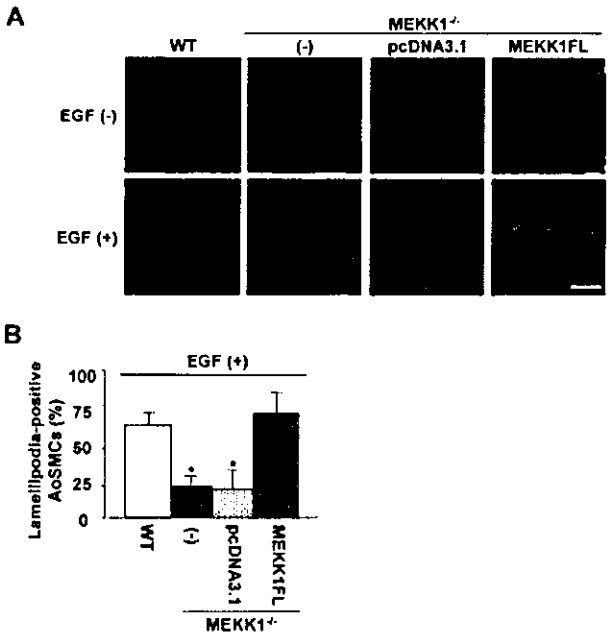

Figure 5. Lamellipodia formation in AoSMCs. A, Representative photomicrographs of lamellipodia formation in AoSMCs with or without EGF stimulation. Bar indicates 25 μm. B, Percentage of lamellipodia-positive cells (n=100) in AoSMCs with EGF. *$P<0.05$ vs WT AoSMCs.

the ligation model because of its excellent reproducibility. To clarify the mechanism(s) of MEKK1 involvement, we first examined cell proliferation within the arterial wall after ligation and found no statistically significant difference in the number of PCNA-positive cells between WT and MEKK1$^{-/-}$ mice. Results from this ligation model are consistent with the fact that MEKK1$^{-/-}$ mice have no overt defects in growth and fertility.[9] There was also no difference in the proliferation of WT and MEKK1$^{-/-}$ AoSMCs evaluated by [^{3}H]thymidine incorporation and cell number. These findings suggest that SMC proliferation might not contribute to the reduced intimal hyperplasia in MEKK1$^{-/-}$ mice. Then we investigated SMC migration and uPA expression, both of which are important factors for intimal hyperplasia.

We demonstrated that there were significantly fewer intimal PCNA-positive cells 7 days after ligation in MEKK1$^{-/-}$ mice than in WT mice. Because PCNA-positive cells are believed to migrate from the media to the intima,[2] this finding suggests that SMC migration is impaired in MEKK1$^{-/-}$ mice. To directly assess the effects of MEKK1 ablation on SMC migration, we used several migration and invasion assays in vitro. We observed comparable migration or invasion of SMCs under control condition between WT and MEKK1$^{-/-}$ AoSMCs; however, significant impairment of migration or invasion was observed after stimulation with FGF-2 in MEKK1$^{-/-}$ AoSMCs, which was restored by addition of full-length MEKK1. These findings indicate that ablation of MEKK1 impairs invasion and migration, both of which may contribute to reduced intimal hyperplasia wherein growth factors may play a vital role.

Lamellipodia formation is essential for cell migration.[13] Exogenous stimuli, such as PDGF or FGF-2, induce lamellipodia formation that can help to complete the first step of the motility cycle.[14,28] Therefore, we examined whether MEKK1 is involved in lamellipodia formation in AoSMCs. Our results showed that the percentage of lamellipodia-positive cells was significantly smaller in MEKK1$^{-/-}$ AoSMCs compared with WT AoSMCs in the presence of EGF. This finding suggests that the impairment of migration in MEKK1$^{-/-}$ AoSMCs may be due to inhibited formation of lamellipodia. Indeed, addition of MEKK1 to MEKK1$^{-/-}$ AoSMCs recovered their capacity to form lamellipodia and migrate. On the other hand, it has been reported that loss of MEKK1 disrupts focal adhesion composition, with decreased vinculin content and focal adhesion kinase (FAK) cleavage.[29] Because disruption of focal adhesion composition will affect cell migration, further investigation will be needed to clarify its role in MEKK1$^{-/-}$ mice.

There is evidence that uPA is induced after arterial injury.[5,28,30,31] uPA enhances vascular remodeling by transforming plasminogen into plasmin, which can activate metalloproteinases and in turn degrade ECM proteins.[5,30,31] We found that uPA expression began to increase at 1 day and reached a peak 3 days after ligation in WT mice, whereas uPA staining appeared to be significantly lower in MEKK1$^{-/-}$ arteries at corresponding times. In vitro, PDGF-BB– and FGF-2–induced uPA expression as detected by immunofluorescence staining and Western blotting was also significantly decreased in MEKK1$^{-/-}$ AoSMCs. Thus, in addition to impaired lamellipodia formation, inhibited uPA expression by MEKK1 ablation may also contribute to impairment of SMC invasion. Addition of full-length MEKK1 restored uPA expression in MEKK1$^{-/-}$ AoSMCs.

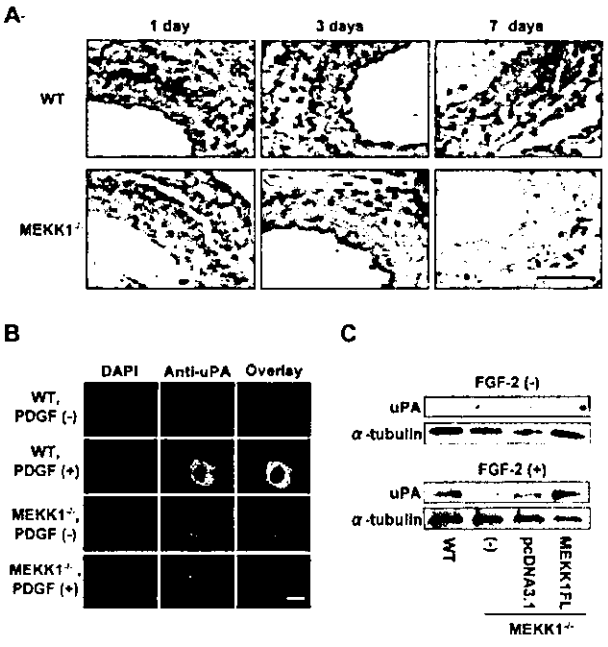

Figure 6. Expression of uPA in AoSMCs. A, Immunohistochemical analysis of time course of uPA expression 1, 3, and 7 days after ligation of carotid arteries. Bar indicates 100 μm. B, Immunofluorescence staining for uPA in AoSMCs stimulated with PDGF-BB. Bar indicates 10 μm. C, Western blots of uPA in AoSMCs stimulated with FGF-2.

Although it has been reported that MEKK1 is required for FGF-2–induced signals to control uPA expression in fibroblasts,[15] further investigations will be needed to elucidate the mechanism by which MEKK1 regulates uPA expression in arteries after ligation.

Recent studies have demonstrated that JNK and ERK transduction pathways may regulate cell migration[32,33] and uPA expression.[34,35] In the present study, we demonstrated that JNK and ERK activation after growth factor stimulation was blunted in MEKK1$^{-/-}$ AoSMCs. Thus, it is possible that ablation of MEKK1 may inhibit cell migration and uPA expression by interfering with the downstream signaling pathways JNK and/or ERK. MEKK1 also has been reported to be associated with cytoskeletal reorganization[11,12] and to be necessary for uPA upregulation,[15] suggesting another possibility that ablation of MEKK1 directly inhibits lamellipodia formation and uPA expression. The stimulus for remodeling after ligation is also influenced by the resultant vascular ischemia. Because MEKK1 is activated by hypoxic stimuli as well as growth factors,[36] we must consider the possibility that the resultant hypoxic stimuli are also important during vascular remodeling in the ligation model.

Izumi et al[22] demonstrated that activation of apoptosis signal–regulating kinase 1 (ASK1), another member of the MAP3K family, also plays a key role during intimal hyperplasia in the carotid artery balloon injury model. Unlike MEKK1, ablation of ASK1 blunted both JNK and p38 but not ERK activation in AoSMCs after serum stimulation. In addition, ablation of ASK1 caused impairment of both SMC migration and proliferation. Thus, although the methods or models used to evaluate functions of MEKK1 and ASK1 were not the same, both MEKK1 and ASK1 may contribute to the development of intimal hyperplasia by different mechanisms.

In conclusion, we have demonstrated that MEKK1 plays a critical role during intimal hyperplasia in a mouse carotid blood-flow cessation model. Intimal hyperplasia is greatly lessened, possibly due to a reduction of SMC invasion by an impairment of their migration and reduced uPA expression. We propose that MEKK1 is a potential target for drug development to prevent vascular remodeling.

Acknowledgments

This study was supported by grants on Human Genome, Tissue Engineering, and Food Biotechnology (H13-genome-11) and grants on Comprehensive Research on Aging and Health [H13-21seiki(seikatsu)-23] in Health and Labor Science Research from the Ministry of Health, Labor, and Welfare, Japan. We thank Hiroko Okuda for technical assistance and Yukari Arino for secretarial work.

References

1. Sakaguchi T, Yan SF, Yan SD, Belov D, Rong LL, Sousa M, Andrassy M, Marso SP, Duda S, Arnold B, Liliensiek B, Nawroth PP, Stern DM, Schmidt AM, Naka Y. Central role of RAGE-dependent neointimal expansion in arterial restenosis. *J Clin Invest*. 2003;111:959–972.
2. Newby AC, Zaltsman AB. Molecular mechanisms in intimal hyperplasia. *J Pathol*. 2000;190:300–309.
3. Maheshwari G, Lauffenburger DA. Deconstructing (and reconstructing) cell migration. *Microsc Res Tech*. 1998;43:358–368.
4. Reidy MA, Irvin C, Lindner V. Migration of arterial wall cells: expression of plasminogen activators and inhibitors in injured rat arteries. *Circ Res*. 1996;78:405–414.
5. Carmeliet P, Moons L, Herbert JM, Crawley J, Lupu F, Lijnen R, Collen D. Urokinase but not tissue plasminogen activator mediates arterial neointima formation in mice. *Circ Res*. 1997;81:829–839.
6. Minamino T, Yujiri T, Terada N, Taffet GE, Michael LH, Johnson GL, Schneider MD. MEKK1 is essential for cardiac hypertrophy and dysfunction induced by Gq. *Proc Natl Acad Sci U S A*. 2002;99:3866–3871.
7. Yujiri T, Sather S, Fanger GR, Johnson GL. Role of MEKK1 in cell survival and activation of JNK and ERK pathways defined by targeted gene disruption. *Science*. 1998;282:1911–1914.
8. Minamino T, Yujiri T, Papst PJ, Chan ED, Johnson GL, Terada N. MEKK1 suppresses oxidative stress–induced apoptosis of embryonic stem cell–derived cardiac myocytes. *Proc Natl Acad Sci U S A*. 1999;96:15127–15132.
9. Yujiri T, Ware M, Widmann C, Oyer R, Russell D, Chan E, Zaitsu Y, Clarke P, Tyler K, Oka Y, Fanger GR, Henson P, Johnson GL. MEK kinase 1 gene disruption alters cell migration and c-Jun NH_2-terminal kinase regulation but does not cause a measurable defect in NF-κB activation. *Proc Natl Acad Sci U S A*. 2000;97:7272–7277.
10. Xia Y, Makris C, Su B, Li E, Yang J, Nemerow GR, Karin M. MEK kinase 1 is critically required for c-Jun *N*-terminal kinase activation by proinflammatory stimuli and growth factor–induced cell migration. *Proc Natl Acad Sci U S A*. 2000;97:5243–5248.
11. Christerson LB, Vanderbilt CA, Cobb MH. MEKK1 interacts with α-actinin and localizes to stress fibers and focal adhesions. *Cell Motil Cytoskeleton*. 1999;43:186–198.
12. Yujiri T, Fanger GR, Garrington TP, Schlesinger TK, Gibson S, Johnson GL. MEK kinase 1 (MEKK1) transduces c-Jun NH_2-terminal kinase activation in response to changes in the microtubule cytoskeleton. *J Biol Chem*. 1999;274:12605–12610.
13. Small JV, Stradal T, Vignal E, Rottner K. The lamellipodium: where motility begins. *Trends Cell Biol*. 2002;12:112–120.
14. DesMarais V, Ichetovkin I, Condeelis J, Hitchcock-DeGregori SE. Spatial regulation of actin dynamics: a tropomyosin-free, actin-rich compartment at the leading edge. *J Cell Sci*. 2002;115:4649–4660.
15. Witowsky J, Abell A, Johnson NL, Johnson GL, Cuevas BD. MEKK1 is required for inducible urokinase-type plasminogen activator expression. *J Biol Chem*. 2003;278:5941–5946.
16. Kumar A, Lindner V. Remodeling with neointima formation in the mouse carotid artery after cessation of blood flow. *Arterioscler Thromb Vasc Biol*. 1997;17:2238–2244.
17. Schafer K, Konstantinides S, Riedel C, Thinnes T, Muller K, Dellas C, Hasenfuss G, Loskutoff DJ. Different mechanisms of increased luminal stenosis after arterial injury in mice deficient for urokinase- or tissue-type plasminogen activator. *Circulation*. 2002;106:1847–1852.
18. Murakoshi N, Miyauchi T, Kakinuma Y, Ohuchi T, Goto K, Yanagisawa M, Yamaguchi I. Vascular endothelin-B receptor system in vivo plays a favorable inhibitory role in vascular remodeling after injury revealed by endothelin-B receptor–knockout mice. *Circulation*. 2002;106:1991–1998.
19. Kuzuya M, Kanda S, Sasaki T, Tamaya-Mori N, Cheng XW, Itoh T, Itohara S, Iguchi A. Deficiency of gelatinase A suppresses smooth muscle cell invasion and development of experimental intimal hyperplasia. *Circulation*. 2003;108:1375–1381.
20. Bradshaw AD, Francki A, Motamed K, Howe C, Sage EH. Primary mesenchymal cells isolated from SPARC-null mice exhibit altered morphology and rates of proliferation. *Mol Biol Cell*. 1999;10:1569–1579.
21. Yujiri T, Nawata R, Takahashi T, Sato Y, Tanizawa Y, Kitamura T, Oka Y. MEK kinase 1 interacts with focal adhesion kinase and regulates insulin receptor substrate-1 expression. *J Biol Chem*. 2003;278:3846–3851.
22. Izumi Y, Kim S, Yoshiyama M, Izumiya Y, Yoshida K, Matsuzawa A, Koyama H, Nishizawa Y, Ichijo H, Yoshikawa J, Iwao H. Activation of apoptosis signal–regulating kinase 1 in injured artery and its critical role in neointimal hyperplasia. *Circulation*. 2003;108:2812–2818.
23. Galis ZS, Johnson C, Godin D, Magid R, Shipley JM, Senior RM, Ivan E. Targeted disruption of the matrix metalloproteinase-9 gene impairs smooth muscle cell migration and geometrical arterial remodeling. *Circ Res*. 2002;91:852–859.
24. Hsieh CC, Lau Y. Migration of vascular smooth muscle cells is enhanced in cultures derived from spontaneously hypertensive rat. *Pflugers Arch*. 1998;435:286–292.

25. Chaulet H, Desgranges C, Renault MA, Dupuch F, Ezan G, Peiretti F, Loirand G, Pacaud P, Gadeau AP. Extracellular nucleotides induce arterial smooth muscle cell migration via osteopontin. *Circ Res.* 2001;89:772–778.
26. Watanabe M, Yano W, Kondo S, Hattori Y, Yamada N, Yanai R, Nishida T. Up-regulation of urokinase-type plasminogen activator in corneal epithelial cells induced by wounding. *Invest Ophthalmol Vis Sci.* 2003;44:3332–3338.
27. Zhang L, Deng M, Kao CW, Kao WW, Xia Y. MEK kinase 1 regulates c-Jun phosphorylation in the control of corneal morphogenesis. *Mol Vis.* 2003;9:584–593.
28. Kessels MM, Engqvist-Goldstein AE, Drubin DG. Association of mouse actin-binding protein 1 (mAbp1/SH3P7), an Src kinase target, with dynamic regions of the cortical actin cytoskeleton in response to Rac1 activation. *Mol Biol Cell.* 2000;11:393–412.
29. Cuevas BD, Abell AN, Witowsky JA, Yujiri T, Johnson NL, Kesavan K, Ware M, Jones PL, Weed SA, DeBiasi RL, Oka Y, Tyler KL, Johnson GL. MEKK1 regulates calpain-dependent proteolysis of focal adhesion proteins for rear-end detachment of migrating fibroblasts. *EMBO J.* 2003;22:3346–3355.
30. Carmeliet P, Moons L, Lijnen R, Baes M, Lemaitre V, Tipping P, Drew A, Eeckhout Y, Shapiro S, Lupu F, Collen D. Urokinase-generated plasmin activates matrix metalloproteinases during aneurysm formation. *Nat Genet.* 1997;17:439–444.
31. Lamfers ML, Lardenoye JH, de Vries MR, Aalders MC, Engelse MA, Grimbergen JM, van Hinsbergh VW, Quax PH. In vivo suppression of restenosis in balloon-injured rat carotid artery by adenovirus-mediated gene transfer of the cell surface-directed plasmin inhibitor ATF.BPTI. *Gene Ther.* 2001;8:534–541.
32. Xia Y, Karin M. The control of cell motility and epithelial morphogenesis by Jun kinases. *Trends Cell Biol.* 2004;14:94–101.
33. Matsubayashi Y, Ebisuya M, Honjoh S, Nishida E. ERK activation propagates in epithelial cell sheets and regulates their migration during wound healing. *Curr Biol.* 2004;14:731–735.
34. Benasciutti E, Pages G, Kenzior O, Folk W, Blasi F, Crippa MP. MAPK and JNK transduction pathways can phosphorylate Sp1 to activate the uPA minimal promoter element and endogenous gene transcription. *Blood.* 2004;104:256–262.
35. Jo M, Thomas KS, O'Donnell DM, Gonias SL. Epidermal growth factor receptor–dependent and –independent cell-signaling pathways originating from the urokinase receptor. *J Biol Chem.* 2003;278:1642–1646.
36. Lee SR, Lo EH. Interactions between p38 mitogen-activated protein kinase and caspase-3 in cerebral endothelial cell death after hypoxia-reoxygenation. *Stroke.* 2003;34:2704–2709.

ELSEVIER

Cardiovascular Research 65 (2005) 879–888

Cardiovascular Research

www.elsevier.com/locate/cardiores

Benidipine, a long-acting calcium channel blocker, inhibits cardiac remodeling in pressure-overloaded mice

Yulin Liao[a], Masanori Asakura[a], Seiji Takashima[a], Akiko Ogai[b], Yoshihiro Asano[a], Hiroshi Asanuma[a], Tetsuo Minamino[a], Hitonobu Tomoike[b], Masatsugu Hori[a], Masafumi Kitakaze[b,*]

[a]*Department of Internal Medicine and Therapeutics, Osaka University Graduate School of Medicine, 2-2 Yamadaoka, Suita, Osaka 565-0781, Japan*
[b]*Cardiovascular Division of Internal Medicine, National Cardiovascular Center (M.K.), 5-7-1 Fujishirodai, Suita, Osaka 565-8565, Japan*

Received 9 August 2004; received in revised form 25 October 2004; accepted 3 November 2004
Available online 24 November 2004
Time for primary review 19 days

Abstract

Objective: The effects of long-acting calcium channel blockers (CCBs) on pressure overload-induced cardiac remodeling are seldom studied in animals. We evaluated the effects of benidipine, a long-acting CCB, on cardiac remodeling.
Methods: Rat neonatal cardiac myocytes were used to examine the influence of benidipine on protein synthesis. Cardiac remodeling was induced in C57 B6/J mice by transverse aortic constriction (TAC). Then the effects of benidipine (10 mg/kg/d) were assessed on myocardial hypertrophy and heart failure, cardiac histology, and gene expression.
Results: Benidipine significantly inhibited protein synthesis by cardiac myocytes stimulated with phenylephrine (PE), and this effect was partially abolished by cotreatment with a nitric oxide synthase (NOS) inhibitor [N(G)-nitro-L-arginine methylester (L-NAME)]. Four weeks after the onset of pressure overload, benidipine therapy potently inhibited cardiac hypertrophy and prevented heart failure. The heart to body weight ratio was 6.89±0.48 mg/g in treated mice vs. 8.76±0.33 mg/g in untreated mice ($P<0.01$), and the lung to body weight ratio was 7.39±0.93 mg/g vs. 10.53±0.99 mg/g, respectively ($P<0.05$). Left ventricular fractional shortening (LVFS) was improved on echocardiography. Plasma NO levels were increased, while B type natriuretic peptide, protein inhibitor of neuronal NOS, and procollagen IV alpha were down-regulated in benidipine-treated mice.
Conclusion: These results indicate that benidipine inhibits cardiac remodeling due to pressure overload at least partly by acting on the nitric oxide signaling pathway.
© 2004 European Society of Cardiology. Published by Elsevier B.V. All rights reserved.

Keywords: Calcium channel blocker; Heart failure; Hypertrophy; Gene expression

1. Introduction

Calcium channel blockers (CCBs) are one of the most frequently used classes of drugs for the treatment of hypertension. Although early clinical studies showed a disappointing outcome when short-acting dihydropyridine CCBs were used to reduce cardiovascular risk [1,2], well-designed prospective randomized controlled clinical trials have demonstrated that long-acting dihydropyridine CCBs are effective for reduction of the blood pressure (BP), inhibition of cardiac remodeling, and decreasing the risk of cardiovascular endpoints [3]. However, the underlying mechanism of the beneficial effect of CCBs on cardiac remodeling is not fully understood. An earlier study performed by our laboratory showed that the vasodilator hydralazine significantly lowered the systemic blood pressure but did not exert any effect on cardiac hypertrophy induced in rats by N(G)-nitro-L-arginine methylester (L-NAME), a nitric oxide (NO) synthase inhibitor [4], suggesting that blood pressure reduction alone was not sufficient to inhibit cardiac remodeling. We also

* Corresponding author. Tel.: +81 6 6833 5012x2225; fax: +81 6 6836 1120.
E-mail address: kitakaze@zf6.so-net.ne.jp (M. Kitakaze).

0008-6363/$ - see front matter © 2004 European Society of Cardiology. Published by Elsevier B.V. All rights reserved.
doi:10.1016/j.cardiores.2004.11.006

reported that a long-acting CCB, benidipine, could increase coronary flow and reduce myocardial ischemia by promoting the release of NO [5,6]. NO is also known to lessen the severity of cardiac hypertrophy and heart failure [7,8]. Furthermore, benidipine has been demonstrated to inhibit myocardial fibrosis in diabetic rats [9]. Based on these lines of evidence, we hypothesized that benidipine may inhibit cardiac remodeling via the NO signaling pathway.

Because the occurrence of cardiac remodeling has been shown to be associated with subsequent cardiovascular events, therapeutic approaches that inhibit cardiac remodeling are likely to improve the prognosis. Chronic left ventricular pressure overload induced by transverse aortic constriction (TAC) is a well established animal model for investigation of cardiac remodeling [10–12], but few experimental studies have attempted to clarify the effects of long-acting CCBs on cardiac remodeling using this model. Therefore, we evaluated the effects of benidipine on cardiac hypertrophy and heart failure in a murine model of pressure overload due to TAC and explored the mechanisms involved.

2. Methods

2.1. Cell culture

Rat neonatal cardiac myocytes were isolated, as described previously [13]. The myocytes were cultured in Dulbecco's modified Eagle's medium (DMEM; Sigma) supplemented with 10% FBS (Equitech-Bio), which was changed to serum-free medium after 72 h. Cells were cultured under serum-free conditions for 48 h before agents were added. Protein synthesis by cultured cells was evaluated from [^{3}H] leucine incorporation, as described elsewhere [11,13]. Cardiac myocytes were exposed to 10^{-4} M phenylephrine (PE) for 24 h in the presence or absence of benidipine (kindly provided by the Pharmaceutical Research Laboratories of Kyowa Hakko Kogyo Sunto, Shizuoka, Japan), and the increase of [^{3}H] leucine uptake was examined. To determine whether the NO signaling pathway was involved in the inhibition of protein synthesis by cardiac myocytes, we examined whether the in vitro effect of benidipine could be blocked by the NO synthase (NOS) inhibitor L-NAME (10^{-5} M).

2.2. Animal model

All procedures were performed in accordance with the Guide for the Care and Use of Laboratory Animals published by the US National Institutes of Health (NIH Publication No. 85–23, revised 1996). Male C57BL/6J mice aged 8–9 weeks and weighing 19–23 g were anesthetized with a mixture of xylazine (5 mg/kg) and ketamine (100 mg/kg) injected intraperitoneally. Then pressure overload was created, as described preciously [10]. Briefly, endotracheal intubation was performed, and the cannula was connected to a volume-cycled rodent ventilator with a tidal volume of 0.5 ml (room air) and a respiration rate of 100/min. The chest was entered via the second intercostal space at the upper left sternal border. After the arch of the aorta was isolated, TAC was created using a 7–0 suture tied twice around a 27-gauge needle and the aortic arch between the innominate and left common carotid arteries. After the suture was tied, the needle was gently removed, yielding 60–80% constriction of the aorta. More than 1000 murine TAC models have been created at our laboratory, and cardiac hypertrophy occurs in 100% of these animals. The dispersion of heart weight to body weight ratio evaluated with statistical parameter coefficient variance at 4 weeks following TAC is about 20%, as we reported previously [11,14].

To test whether benidipine could inhibit the cardiac hypertrophy due to TAC, we treated the mice with either saline (TAC group) or benidipine at 10 mg/kg/d (po, mixed with 0.3% carboxymethyl cellulose sodium and suspended in water) from the 2nd day after surgery. The benidipine dose was based on previous reports from our [4] and another [9] laboratory as well as a preliminary study. To confirm that the extent of the pressure overload was similar between benidipine-treated and untreated animals, three mice were randomly selected from each group to measure the pressure in ascending aorta, using a 1.4 F Millar Pressure Catheter on the 2nd day after TAC. Four weeks after the creation of pressure overload, both the tail cuff blood pressure (BP) and the heart rate (HR; BP-98A, Softron, Tokyo, Japan) were measured 1 day before sacrifice. LV hemodynamic studies were performed by cannulation of the right carotid artery with a Millar Pressure Catheter that was carefully advanced to the LV. Then the mice were killed to measure organ weights and to perform histological analysis.

2.3. Histological examination

The cross-sectional area of cardiac myocytes and the extent of myocardial fibrosis were measured, as described elsewhere [4,15]. Briefly, the cardiac myocyte area and myocardial fibrosis area were analyzed quantitatively by morphometry of either HE-stained or Azan/Mallory-stained sections. The original images were digitized and transformed into binary images, after which the cardiac myocyte area or fibrosis area was calculated with an automatic area quantification program (NIH Image). One hundred myocytes per heart were counted, and the average value was determined. The total myocardial fibrosis index was defined as the sum of the total area of fibrosis in the entire microscopic field divided by the sum of total connective tissue area plus the myocardial area in the entire field.

2.4. Echocardiography

Transthoracic echocardiography was performed with a Sonos 4500 and a 15–6 L MHz transducer (Philips, the Netherlands). Mice were weighed, lightly anesthetized with

2.5% avertin (0.06 ml/10 g), and set in the left lateral decubitus position or the supine position. After the mouse recovered to complete consciousness (about 10 min), two-dimensional short-axis views of the left ventricle were obtained for guided M-mode measurement of the left ventricular diastolic posterior wall thickness (LVPWd), left ventricular end-diastolic dimension (LVEDd), and left ventricular end-systolic dimension (LVESd). Left ventricular fractional shortening (LVFS) was calculated as follows: LVFS=(LVEDd−LVESd)/LVEDd*100.

2.5. Microarray analysis

To determine the gene expression profile during cardiac remodeling, we performed microarray studies of murine hearts after pressure overload for 1 or 4 weeks. Data about the time course of the induction of NO synthase and fibrosis-related genes were needed to investigate their roles in cardiac hypertrophy and heart failure. Total RNA was prepared from murine hearts using Triazol (Gibco-BRL), according to the manufacturer's instructions. Microarray hybridization was performed in duplicate using Affymetrix Murine Genome U74v2A gene chips and RNA from hearts of animals in the TAC or sham operation groups at 1 or 4 weeks after surgery. Data were analyzed using Genespring 6 software [16].

2.6. Measurement of plasma nitric oxide

Blood was obtained from the right ventricle with a 23-gauge needle at the time of sacrificing the mice. The plasma concentrations of NOx (NO_2+NO_3) was measured with an autoanalyzer (ENO-10, Eicom Kyoto, Japan), as described elsewhere [5,6,17]. Samples were applied to an analytical column that was connected to a copperized cadmium reduction column to reduce NO_2 to NO_3, which was then reacted with Griess reagent, and the absorbance of the product was measured at 540 nm.

2.7. Quantitative PCR

Based on the results of microarray analysis, we chose three genes that were consistently up-regulated at both 1 and 4 weeks after the onset of LV pressure overload and were closely related to cardiac hypertrophy or heart failure. We further investigated the effects of benidipine on these genes by real-time PCR. The three genes were the natriuretic peptide precursor type B (BNP) gene, protein inhibitor of neuronal nitric oxide synthase (PIN) gene, and procollagen IV alpha gene. Primers were designed using Gene Express software. Using 50 ng/μl of total RNA as the template, quantitative measurement was performed with an ABI Prism 7700 sequencing system. Amplification was done by the one-step method using a Quantitect SYBR Green RT-PCR kit (QIAGEN). Glyceraldehyde-3-phosphate dehydrogenase (GAPDH) was amplified as an endogenous control, and quantitation of target gene levels was performed relative to this gene.

2.8. Statistical analysis

For all statistical tests, multiple comparison was performed by one-way ANOVA with the Tukey–Kramer exact probability test. The least-squares method was used for linear correlation between selected variables. Results are reported as the mean±S.E.M., and $P<0.05$ was considered statistically significant.

3. Results

3.1. Benidipine reduces cardiac myocyte protein synthesis stimulated by PE

Benidipine (10^{-4} M) did not affect basal [^{3}H] leucine uptake by cardiac myocytes, but it inhibited PE-induced

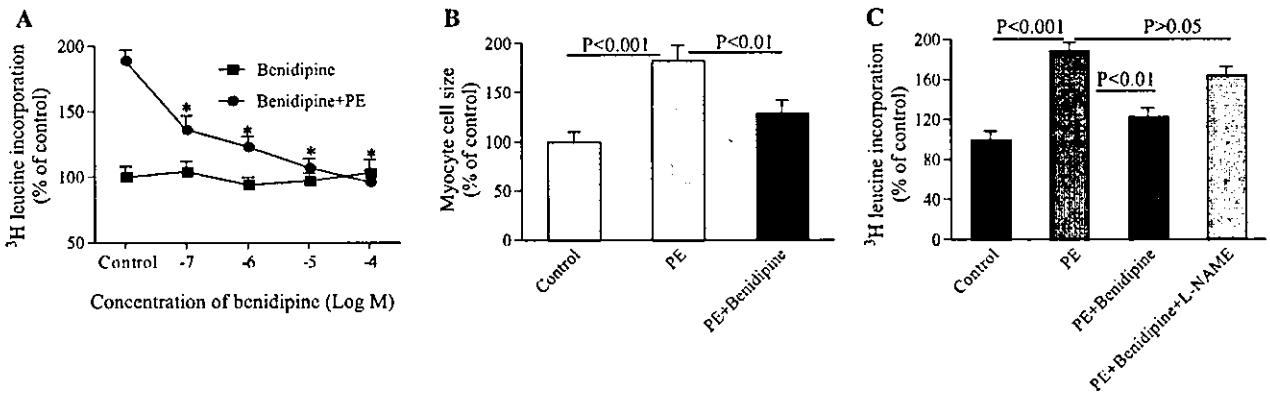

Fig. 1. Effect of benidipine on protein synthesis and the size of neonatal rat cardiac myocytes. (A) Protein synthesis stimulated by 10^{-4} M phenylephrine (PE) was inhibited by benidipine at concentrations ranging from 10^{-7}–10^{-4} M in a dose-independent fashion, and this concentration range did not affect normal cardiac myocytes. *$P<0.01$ vs. control. (B) The cell size was calculated from 200 cells in every group. The increase of cell size caused by PE (10^{-4} M) was inhibited by treatment with benidipine (10^{-5} M). (C) The inhibitory effect of benidipine (10^{-5} M) on protein synthesis induced by PE was partially blocked by cotreatment with L-NAME (10^{-5} M).

Table 1
Hemodynamic and echocardiographic data obtained at 4 weeks

Group	BW (g)	HR (bpm)	SBP (mm Hg)	LVPWd (mm)	LVEDd (mm)	LVESd (mm)
Sham	25.2±0.4**	651±11	114±3	0.65±0.02***	3.07±0.06	1.64±0.04**
TAC	22.64±0.41	686±26	101±5	0.98±0.04	3.38±0.12	2.29±0.04
TAC+Beni	23.1±0.4	652±26	105±2	0.77±0.03***	3.04±0.06*	1.69±0.12**

Beni—benidipine (10 mg/kg/d po); BW—body weight; HR—heart rate; SBP—Tail cuff systolic blood pressure; LVPWd—LV diastolic posterior wall thickness; LVEDd—LV end-diastolic dimension; LVESd—left ventricular end-systolic dimension. The number of mice in the sham, TAC, and TAC+benidipine groups was 10, 17, and 11, respectively, for BW, LVPWd, LVEDd, and LVESd; and 10, 9, and 7 for HR and SBP.

* $P<0.05$.

** $P<0.01$.

*** $P<0.001$ vs. TAC (transverse aortic constriction).

protein synthesis in a concentration-dependent fashion (Fig. 1A). The enlargement of cells induced by PE was also inhibited by benidipine (Fig. 1B). The inhibitory effect of benidipine on PE-induced protein synthesis was partially blocked by L-NAME (Fig. 1C).

3.2. Benidipine inhibits pathological cardiac hypertrophy

The hemodynamic and echocardiographic data obtained just before sacrifice are shown in Table 1. Benidipine (10 mg/kg/d) did not significantly affect the tail cuff systolic blood pressure, but the LV wall was thinner, and LV dimensions were smaller in benidipine-treated mice than in TAC mice (Table 1).

Echocardiography and hemodynamics showed no differences among the three groups of mice before surgery (data not shown). The ascending aortic systolic blood pressure was measured on the 2nd day after TAC or sham operation without drug treatment in order to evaluate the extent of pressure overload (in three mice per group), no significant difference was noted between the TAC and benidipine groups (98±5 mm Hg in the sham group, 163±4 mm Hg in the TAC group, and 161±3 mm Hg in the benidipine group).

LV hemodynamics were similar between TAC mice with or without benidipine treatment (Fig. 2), suggesting that an oral dose of 10 mg/kg did not significantly affect LV function.

Consistent with the in vitro results, benidipine markedly inhibited cardiac hypertrophy at 4 weeks after TAC (Fig. 3). Histological examination showed that the extent of myocyte hypertrophy (Fig. 4A,B) was reduced and that myocardial fibrosis was less severe in benidipine-treated mice (Fig. 4C,D).

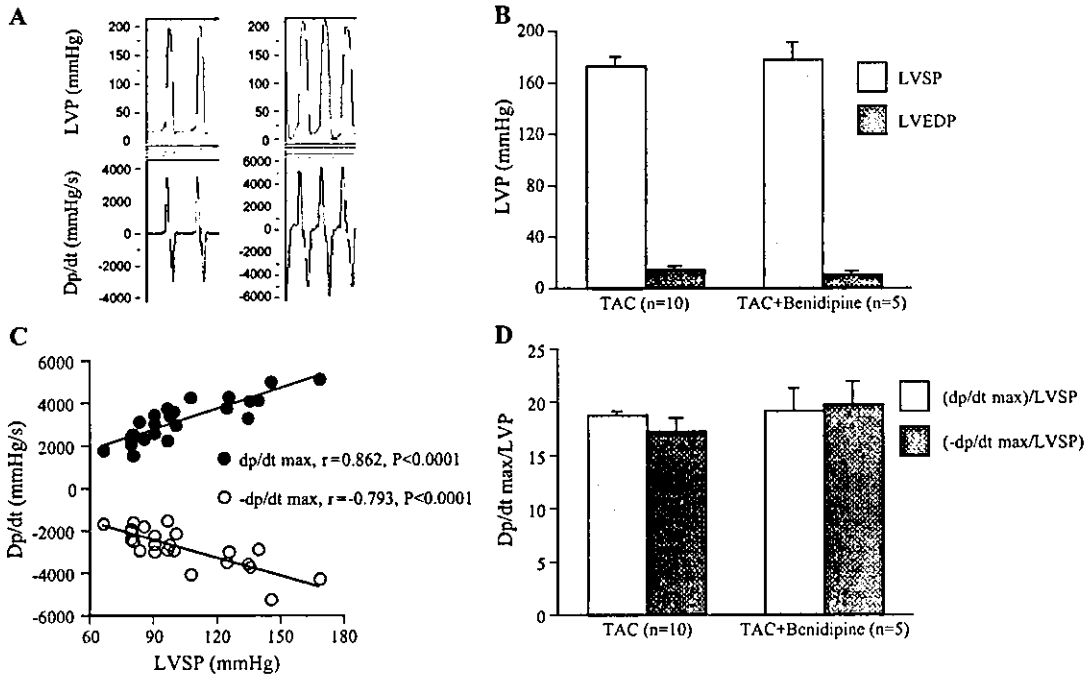

Fig. 2. Left ventricular (LV) hemodynamics measured with a Millar Catheter at 4 weeks after TAC. (A) LV pressure and dp/dt in the TAC and benidipine groups. (B) No significant differences of LV systolic pressure (LVSP) and LV end-diastolic pressure (LVEDP) were noted between TAC mice with or without benidipine. (C) ±Dp/dt max was closely correlated with LVSP in untreated mice. (D) ±Dp/dt max/LVSP was not significantly increased in benidipine-treated mice.

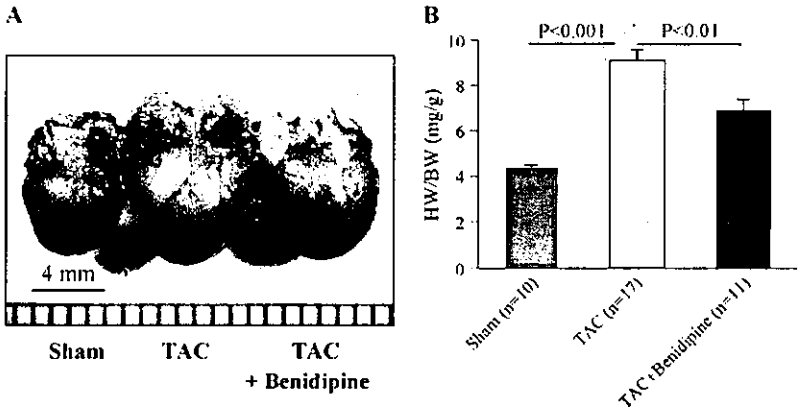

Fig. 3. Benidipine inhibits cardiac remodeling. (A) Representative pictures of whole hearts. (B) The heart to body weight ratio (HW/BW) was significantly decreased in TAC mice treated with benidipine (10 mg/kg/d) compared with untreated TAC mice.

3.3. Benidipine prevents progression from hypertrophy to heart failure

TAC induced congestive heart failure with a reduction in LVFS and increase of pulmonary congestion. LVFS measured by echocardiography was significantly higher in benidipine-treated mice than in TAC mice (Fig. 5A,B). Compared with the value for sham-operated mice, the lung weight to body weight ratio (LW/BW) was increased by about 108% in TAC mice, but only rose by 46% in benidipine-treated mice (Fig. 5C,D).

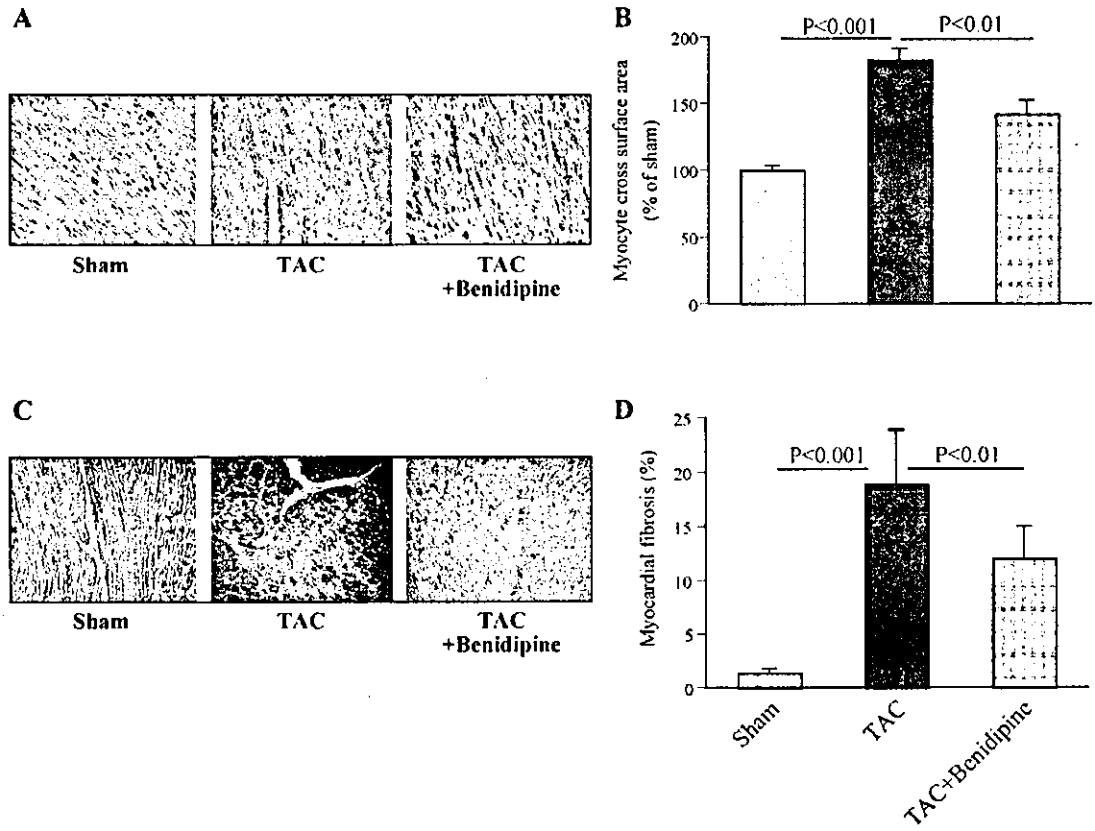

Fig. 4. Results of histological examination. (A) Representative images of the myocardium (HE stain×200). (B) The cross-sectional area of cardiac myocytes was significantly increased in TAC mice by pressure overload for 4 weeks, while treatment with benidipine blunted the enlargement of myocytes. (C) Representative pictures of myocardial fibrosis (Azan–Mallory stain×100). (D) Quantitative analysis showed that benidipine significantly inhibited myocardial fibrosis due to pressure overload for 4 weeks. Three hearts per group were used to determine the cross-sectional area of cardiac myocytes and the extent of myocardial fibrosis.

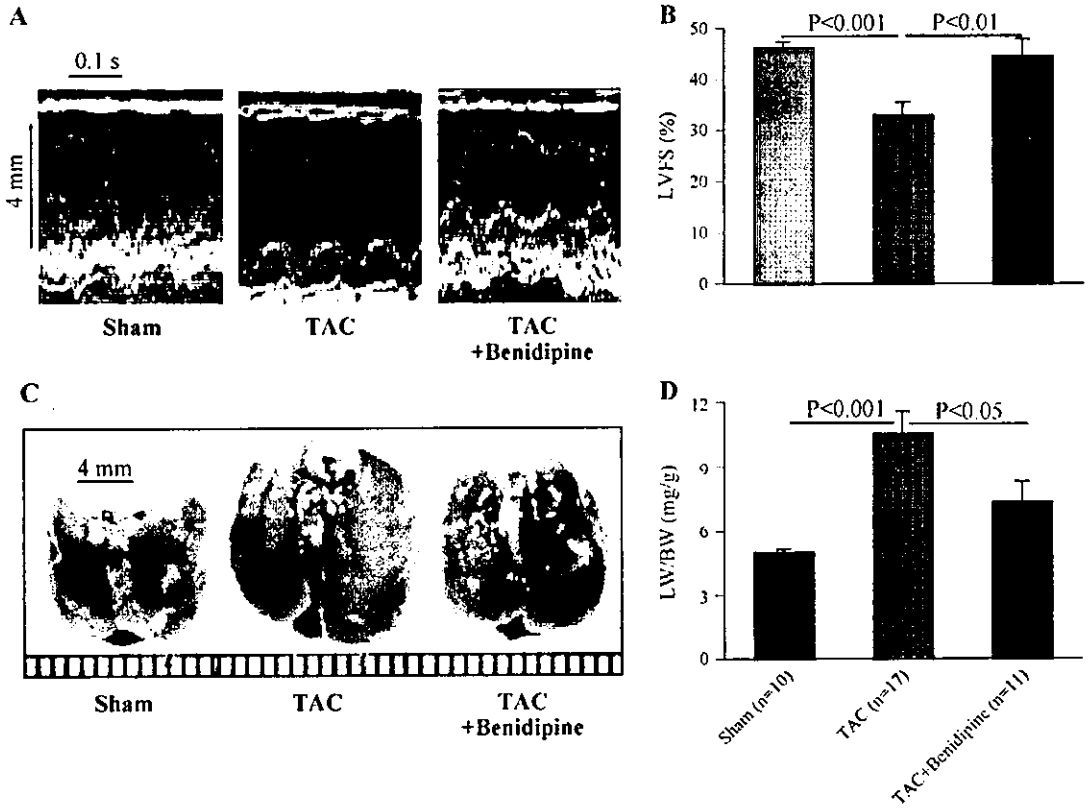

Fig. 5. Benidipine ameliorates heart failure induced by pressure overload. (A) Representative images obtained by echocardiography. (B) LV fractional shortening (LVFS) was increased by benidipine treatment. (C) Macroscopic views of lungs from each group. (D) The lung to body weight ratio (LW/BW) was significantly decreased in TAC mice treated with benidipine in comparison with untreated mice.

3.4. BNP, PIN, and procollagen IV are up-regulated in cardiac hypertrophy

Based on evidence from our laboratory and other investigators that BNP is an important molecular marker of cardiac hypertrophy or heart failure, and that both NO and fibrosis play an important role in cardiac remodeling, we assessed the expression of the BNP, PIN, and procollagen IV alpha genes in pressure-overloaded murine hearts, using microarray analysis. We found that a series of hypertrophy-related genes were up-regulated (Fig. 6A), including the BNP, PIN, and procollagen IV alpha genes, which were consistently up-regulated at both 1 and 4 weeks after TAC. Expression of calmodulin and five other procollagen genes was also increased by pressure overload (Fig. 6B).

3.5. Benidipine increases plasma NOx and down-regulates BNP, PIN, and procollagen IV alpha

As shown in Fig. 7A, the plasma level of NOx was markedly decreased in TAC mice at 4 weeks and was significantly increased in TAC mice treated with benidipine. Quantitative RT-PCR (Fig. 7B–D) demonstrated that benidipine decreased the level of BNP, a molecular marker for hypertrophy, and also down-regulated the expression of PIN and procollagen IV alpha$_1$. These changes supported our other findings in vitro and in vivo that benidipine inhibits cardiac hypertrophy and improves cardiac function partly by increasing the release of NO.

4. Discussion

4.1. Major findings

The present study is the first to evaluate the inhibitory effect of benidipine on cardiac remodeling induced by TAC in mice. The major findings of this study include the observations that (1) benidipine inhibits the increase of protein synthesis by cardiac myocyte stimulated by phenylephrine; (2) cardiac hypertrophy, myocardial fibrosis, and heart failure in pressure-overload mice were ameliorated by treatment with benidipine; and (3) an NO synthase inhibitor partially blocked the beneficial effect of benidipine on myocyte hypertrophy, while benidipine down-regulated protein inhibitor of neuronal nitric oxide synthase and increased the plasma NO level. These findings suggest that benidipine improves cardiac remodeling via an effect on the NO signaling pathway.

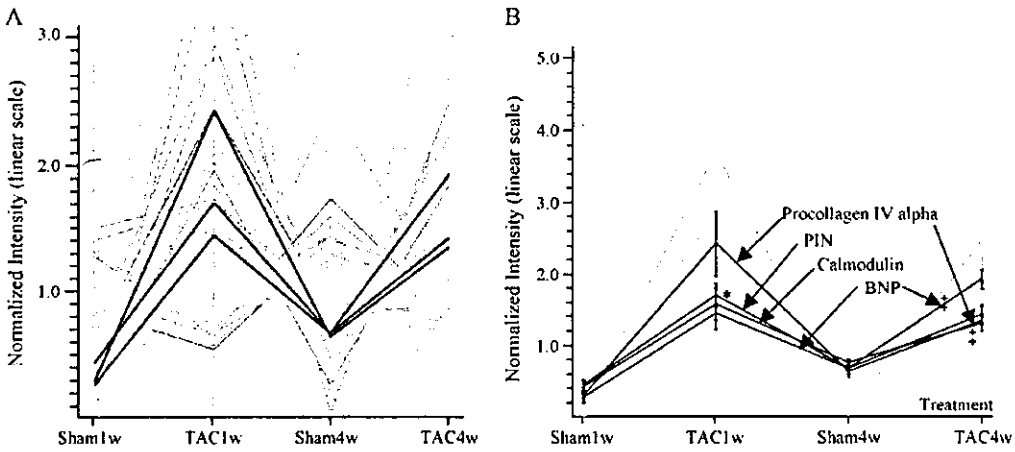

Fig. 6. cDNA microarray analysis of pressure-overload or sham-operated murine hearts. (A) From a total of 12,488 genes, three target genes were selected. These genes were functionally related to cardiac hypertrophy, heart failure, and nitric oxide signaling or fibrosis. (B) The three target genes were significantly up-regulated at 1 and 4 weeks after TAC relative to the levels in corresponding sham mice. Calmodulin and five other procollagen genes also showed up-regulation in response to pressure overload. The number of mice tested in each group was two. *$P<0.05$ vs. sham at 1w, ‡$P<0.05$ vs. sham at 4W (ANOVA).

4.2. Role of NO in cardiac remodeling

NO has been recognized as an important regulator of cardiac remodeling since it can influence both cardiac hypertrophy and heart failure. NO has been reported to exert an antihypertrophic effect in the hearts of spontaneously hypertensive rats without changing the blood pressure [18], which is in agreement with the results of this study. It is generally recognized that hemodynamic factors regulate cardiac myocyte hypertrophy [19], but exceptions have also been frequently reported. We previously reported that hydralazine significantly reduces the systemic blood pressure but does not have any effect on cardiac hypertrophy. In contrast, some drugs inhibit cardiac myocyte hypertrophy in the absence of a significant effect on hemodynamic, as we have reported previously [11,12,14]. Exogenous NO has

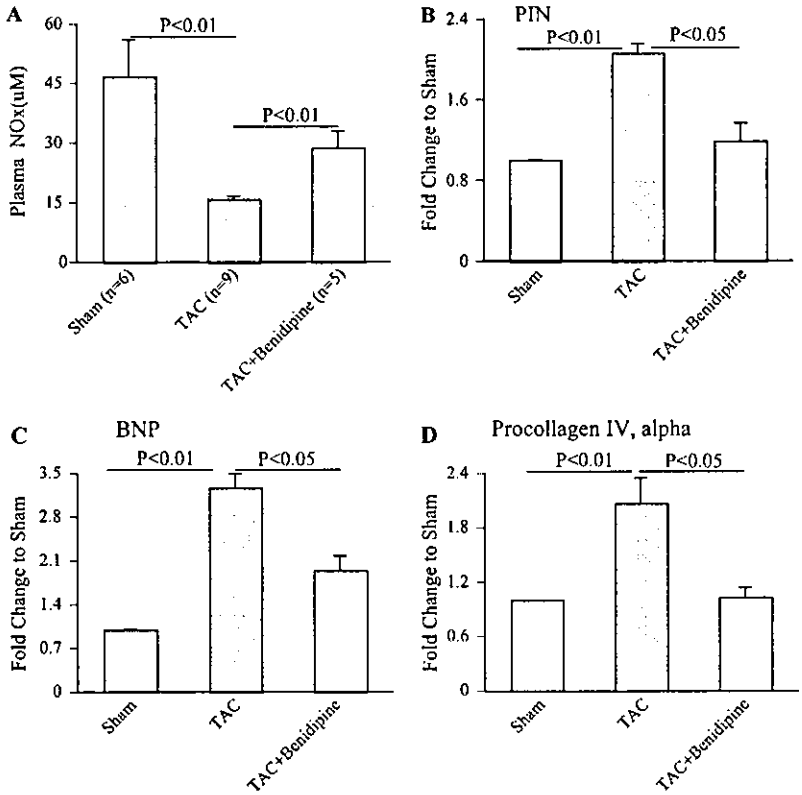

Fig. 7. Plasma nitric oxide level (A) and real-time PCR of the three target genes (B–D). Glyceraldehyde-3-phosphate dehydrogenase (GAPDH) was used as an endogenous control. PIN—protein inhibitor of neuronal nitric oxide synthase; BNP—natriuretic peptide precursor type B. $n=4$ per group for real-time PCR.

also been demonstrated to cause dose-dependent inhibition of alpha$_1$-adrenoceptor-stimulated protein synthesis in neonatal rat myocytes [7]. These results support our finding that benidipine caused a concentration-dependent decrease of PE (an alpha$_1$-adrenoceptor agonist)-stimulated protein synthesis by cardiac myocytes, and that this effect was blunted by NO synthase inhibitor. In addition, benidipine attenuated cardiac hypertrophy in pressure-overload mice without a significant change of blood pressure, and this antihypertrophic effect was at least partially mediated via the down-regulation of myocardial PIN. PIN has been demonstrated to regulate three types of NO synthase (NOS) [20]. Since both neural NOS (nNOS) and endothelial NOS (eNOS) are constitutively expressed in the myocardium, consistent up-regulation of PIN during the progression of cardiac hypertrophy, as noted in this study, is likely to decrease the release of NO. Interestingly, our data showed that benidipine significantly increased circulating NO levels, providing direct evidence for the abovementioned hypothesis that NO may play an important role in regulating cardiac hypertrophy. Although we did not monitor the blood concentration of benidipine, the dose that we used was effective for increasing the production of NO and consequently for attenuating cardiac hypertrophy.

We also found that benidipine could ameliorate progression from cardiac hypertrophy to heart failure, as confirmed by echocardiography, assessment of pulmonary congestion, and measurement of BNP expression. These results are partially attributable to the increase in NO production. Indeed, we have previously reported that benidipine increases coronary blood flow and reduces the severity of myocardial ischemia via an NO-dependent mechanism [5], and benidipine also improves cardiac remodeling induced by the eNOS inhibitor L-NAME [4]. Studies using genetically engineered mice have provided substantial evidence for a critical role of NO in cardiac remodeling. After myocardial infarction, LV dilation is more marked, heart function is more severely impaired, and long-term mortality is higher in eNOS-deficient mice compared with wild-type mice [8]. In contrast, congestive heart failure is less severe, and survival is increased in eNOS transgenic mice receiving coronary ligation [21]. It is worth noting that the preventive effect of benidipine on progression to heart failure may be secondary to its antihypertrophic effect. Further studies are needed to examine whether benidipine is effective in animals or humans with chronic heart failure.

4.3. Fibrosis and cardiac remodeling

Fibrosis of the myocardium plays a pivotal role in the process of cardiac remodeling. In the present study, we found that benidipine could significantly inhibit myocardial fibrosis in pressure-overload mice, a result that agrees with previous findings [9]. Although collagen type I and collagen type III produced by cardiac fibroblasts are the major components of the myocardial collagen matrix, type IV collagen is also expressed by both cardiac myocytes and fibroblasts and is a major component of the basement membrane [22,23]. Type IV collagen was reported to be increased in the hearts of diabetic rat [24] and is found in the fibrotic cardiac lesions of patients with DCM [25]. The angiotensin II-induced increase of fibronectin mRNA in the myocardium is accompanied by a similar increase of type I collagen, type IV collagen, and atrial natriuretic factor steady-state mRNA [26]. In this study, cDNA microarray analysis showed significant up-regulation of procollagen IV alpha at both 1 and 4 weeks after TAC, suggesting that this may be a potentially important gene in cardiac remodeling. Down-regulation of this gene by benidipine might have made an important contribution to the inhibition of cardiac remodeling.

4.4. Benidipine and cardiac sympathetic activity

Long-term cardiac sympathetic activation is detrimental to the heart, so one of the major aims of antihypertensive therapy is to reduce sympathetic tone. Differences in the formulations and pharmacokinetics of CCBs have various clinical influences, altering the effect of these drugs on blood pressure, heart rate, and cardiac sympathetic activity. Short-acting dihydropyridine CCBs enhance noradrenaline release from the sympathetic nerves [27]. In contrast, evidence suggests that long-acting calcium antagonists do not significantly affect sympathetic tone and may exert a more favorable clinical effect [28–30]. Our data showed that benidipine did not increase the heart rate. Moreover, benidipine prevented progression from cardiac hypertrophy to failure, suggesting that it does not enhance sympathetic tone. It is even possible that benidipine counteracts sympathetic activation in cardiac hypertrophy by increasing the release of NO because a reduced action of NO often contributes to overall sympathetic excitation in heart failure (review [31]).

4.5. Perspectives

In summary, this study provided evidence of the beneficial effect of a long-acting calcium antagonist, benidipine, on cardiac remodeling. Benidipine inhibited cardiac myocyte hypertrophy both in vitro and in vivo and also inhibited progression from cardiac hypertrophy to failure due to LV pressure overload. These effects were potentially mediated via an influence on the NO signaling pathway.

The question of whether CCB therapy increases cardiovascular events has attracted worldwide attention. Recent clinical trials have largely settled this question [29,30,32], but CCBs are still linked with a slightly increased risk of heart failure. However, the PRAISE trial revealed that amlodipine, a long-acting CCB, was not associated with increased mortality or morbidity in patients with severe

CHF [29]. Our studies and other investigations have consistently confirmed that amlodipine increases NO production [4,10,33,34]. Benidipine may also be beneficial for patients with hypertension-induced CHF, but a well-designed clinical trial is needed to investigate this point.

Acknowledgement

This work was supported by a Research Grant for Sensory and Communicative Disorders (H14-tokushitsu-38) from the Japanese Ministry of Health and Labor and Welfare.

References

[1] Psaty BM, Heckbert SR, Koepsell TD, Siscovick DS, Raghunathan TE, Weiss NS, et al. The risk of myocardial infarction associated with antihypertensive drug therapies. JAMA 1995;274:620–5.
[2] Furberg CD, Psaty BM, Meyer JV, Nifedipine: Dose-related increase in mortality in patients with coronary heart disease. Circulation 1995;92:1326–31.
[3] Muntwyler J, Follath F. Calcium channel blockers in treatment of hypertension. Prog Cardiovasc Dis 2001;44:207–16.
[4] Sanada S, Node K, Minamino T, Takashima S, Ogai A, Asanuma H, et al. Long-acting Ca2+ blockers prevent myocardial remodeling induced by chronic NO inhibition in rats. Hypertension 2003;41: 963–7.
[5] Kitakaze M, Node K, Minamino T, Asanuma H, Kuzuya T, Hori M. A Ca channel blocker, benidipine, increases coronary blood flow and attenuates the severity of myocardial ischemia via NO-dependent mechanisms in dogs. J Am Coll Cardiol 1999;33:242–9.
[6] Asanuma H, Kitakaze M, Node K, Takashima S, Sakata Y, Asakura M, et al. Benidipine, a long-acting Ca channel blocker, limits infarct size via bradykinin- and NO-dependent mechanisms in canine hearts. Cardiovasc Drugs Ther 2001;15:225–31.
[7] Calderone A, Thaik CM, Takahashi N, Chang DL, Colucci WS. Nitric oxide, atrial natriuretic peptide, and cyclic GMP inhibit the growth-promoting effects of norepinephrine in cardiac myocytes and fibroblasts. J Clin Invest 1998;101:812–8.
[8] Scherrer-Crosbie M, Ullrich R, Bloch KD, Nakajima H, Nasseri B, Aretz HT, et al. Endothelial nitric oxide synthase limits left ventricular remodeling after myocardial infarction in mice. Circulation 2001; 104:1286–91.
[9] Jesmin S, Sakuma I, Hattori Y, Fujii S, Kitabatake A. Long-acting calcium channel blocker benidipine suppresses expression of angiogenic growth factors and prevents cardiac remodelling in a type II diabetic rat model. Diabetologia 2002;45:402–15.
[10] Liao Y, Ishikura F, Beppu S, Asakura M, Takashima S, Asanuma H, et al. Echocardiographic assessment of LV hypertrophy and function in aortic-banded mice: necropsy validation. Am J Physiol, Heart Circ Physiol 2002;282:H1703–8.
[11] Liao Y, Takashima S, Asano Y, Asakura M, Ogai A, Shintani Y, et al. Activation of adenosine A1 receptor attenuates cardiac hypertrophy and prevents heart failure in murine left ventricular pressure-overload model. Circ Res 2003;93:759–66.
[12] Takemoto M, Node K, Nakagami H, Liao Y, Grimm M, Takemoto Y, et al. Statins as antioxidant therapy for preventing cardiac myocyte hypertrophy. J Clin Invest 2001;108:1429–37.
[13] Asakura M, Kitakaze M, Takashima S, Liao Y, Ishikura F, Yoshinaka T, et al. Cardiac hypertrophy is inhibited by antagonism of ADAM12 processing of HB-EGF: metalloproteinase inhibitors as a new therapy. Nat Med 2002;8:35–40.
[14] Liao Y, Asakura M, Takashima S, Ogai A, Asano Y, Shintani Y, et al. Celiprolol, a vasodilatory beta-blocker, inhibits pressure overload-induced cardiac hypertrophy and prevents the transition to heart failure via nitric oxide-dependent mechanisms in mice. Circulation 2004;110:692–9.
[15] Kurisu S, Ozono R, Oshima T, Kambe M, Ishida T, Sugino H, et al. Cardiac angiotensin II type 2 receptor activates the kinin/NO system and inhibits fibrosis. Hypertension 2003;41:99–107.
[16] Asano Y, Takashima S, Asakura M, Shintani Y, Liao Y, Minamino T, et al. Lamr1 functional retroposon causes right ventricular dysplasia in mice. Nat Genet 2004;36:123–30.
[17] Tatsumi T, Akashi K, Keira N, Matoba S, Mano A, Shiraishi J, et al. Cytokine-induced nitric oxide inhibits mitochondrial energy production and induces myocardial dysfunction in endotoxin-treated rat hearts. J Mol Cell Cardiol 2004;37:775–84.
[18] Matsuoka H, Nakata M, Kohno K, Koga Y, Nomura G, Toshima H, et al. Chronic L-arginine administration attenuates cardiac hypertrophy in spontaneously hypertensive rats. Hypertension 1996;27:14–8.
[19] Burlew BS, Weber KT. Connective tissue and the heart. Functional significance and regulatory mechanisms. Cardiol Clin 2000;18: 435–42.
[20] Hemmens B, Woschitz S, Pitters E, Klosch B, Volker C, Schmidt K, et al. The protein inhibitor of neuronal nitric oxide synthase (PIN): characterization of its action on pure nitric oxide synthases. FEBS Lett 1998;430:397–400.
[21] Jones SP, Greer JJ, van Haperen R, Duncker DJ, De Crom R, Lefer DJ. Endothelial nitric oxide synthase overexpression attenuates congestive heart failure in mice. Proc Natl Acad Sci U S A 2003; 100:4891–6.
[22] Murakami M, Kusachi S, Nakahama M, Naito I, Murakami T, Doi M, et al. Expression of the alpha 1 and alpha 2 chains of type IV collagen in the infarct zone of rat myocardial infarction. J Mol Cell Cardiol 1998;30:1191–202.
[23] Chapman D, Weber KT, Eghbali M. Regulation of fibrillar collagen types I and III and basement membrane type IV collagen gene expression in pressure overloaded rat myocardium. Circ Res 1990; 67:787–94.
[24] Doi K, Sawada F, Toda G, Yamachika S, Seto S, Urata Y, et al. Alteration of antioxidants during the progression of heart disease in streptozotocin-induced diabetic rats. Free Radic Res 2001;34:251–61.
[25] Watanabe T, Kusachi S, Yamanishi A, Kumashiro H, Nunoyama H, Sano I, et al. Localization of type IV collagen alpha chain in the myocardium of dilated and hypertrophic cardiomyopathy. Jpn Heart J 1998;39:753–62.
[26] Crawford DC, Chobanian AV, Brecher P. Angiotensin II induces fibronectin expression associated with cardiac fibrosis in the rat. Circ Res 1994;74:727–39.
[27] Hamada T, Watanabe M, Kaneda T, Ohtahara A, Kinugawa T, Hisatome I, et al. Evaluation of changes in sympathetic nerve activity and heart rate in essential hypertensive patients induced by amlodipine and nifedipine. J Hypertens 1998;16:111–8.
[28] Zanchetti A, Bond MG, Hennig M, Neiss A, Mancia G, Dal Palu C, et al. Calcium antagonist lacidipine slows down progression of asymptomatic carotid atherosclerosis: principal results of the European Lacidipine Study on Atherosclerosis (ELSA), a randomized, double-blind, long-term trial. Circulation 2002;106:2422–7.
[29] Packer M, O'Connor CM, Ghali JK, Pressler ML, Carson PE, Belkin RN, et al. Prospective Randomized Amlodipine Survival Evaluation Study Group. Effect of amlodipine on morbidity and mortality in severe chronic heart failure. N Engl J Med 1996;335:1107–14.
[30] Major outcomes in high-risk hypertensive patients randomized to angiotensin-converting enzyme inhibitor or calcium channel blocker vs. diuretic: the Antihypertensive and Lipid-Lowering Treatment to Prevent Heart Attack Trial (ALLHAT). JAMA 2002;288:2981–97.
[31] Li YF, Patel KP. Paraventricular nucleus of the hypothalamus and elevated sympathetic activity in heart failure: the altered inhibitory mechanisms. Acta Physiol Scand 2003;177:17–26.

[32] Hansson L, Lindholm LH, Ekbom T, Dahlof B, Lanke J, Schersten B, et al. Randomised trial of old and new antihypertensive drugs in elderly patients: cardiovascular mortality and morbidity the Swedish Trial in Old Patients with Hypertension-2 study. Lancet 1999;354: 1751–6.

[33] Asano Y, Kim J, Ogai A, Takashima S, Shintani Y, Minamino T, et al. A calcium channel blocker activates both ecto-5(′)-nucleotidase and NO synthase in HUVEC. Biochem Biophys Res Commun 2003; 311:625–8.

[34] Lenasi H, Kohlstedt K, Fichtlscherer B, Mulsch A, Busse R, Fleming I. Amlodipine activates the endothelial nitric oxide synthase by altering phosphorylation on Ser1177 and Thr495. Cardiovasc Res 2003;59:844–53.

Available online at www.sciencedirect.com
SCIENCE DIRECT®
Biochemical and Biophysical Research Communications 327 (2005) 1083–1087
BBRC
www.elsevier.com/locate/ybbrc

Amlodipine ameliorates myocardial hypertrophy by inhibiting EGFR phosphorylation

Yulin Liao[a], Masanori Asakura[a], Seiji Takashima[a], Hisakazu Kato[a], Yoshihiro Asano[a], Yasunori Shintani[a], Tetsuo Minamino[a], Hitonobu Tomoike[b], Masatsugu Hori[a], Masafumi Kitakaze[b,*]

[a] *Department of Internal Medicine and Therapeutics, Osaka University Graduate School of Medicine, 2-2 Yamadaoka, Suita, Osaka 565-0781, Japan*
[b] *Cardiovascular Division of Internal Medicine, National Cardiovascular Center, 5-7-1 Fujishirodai, Suita, Osaka 565-8565, Japan*

Received 7 December 2004
Available online 29 December 2004

Abstract

The effects of long-acting calcium channel blockers on pressure overload-induced cardiac hypertrophy have been little studied in experimental animals and the underlying mechanisms are not fully understood. We previously reported that cardiomyocyte hypertrophy could be induced via phosphorylation of the epidermal growth factor receptor (EGFR). In this study, we investigated whether amlodipine attenuates cardiac hypertrophy by inhibiting EGFR phosphorylation. We found that amlodipine dose-dependently inhibited epinephrine-induced protein synthesis and EGFR phosphorylation in cultured neonatal rat cardiomyocytes. Our in vivo study revealed that amlodipine could ameliorate myocardial hypertrophy induced by transverse aortic constriction (TAC) in C57/B6 mice. One week after TAC, amlodipine treatment (3 mg/kg/day) significantly reduced the heart-to-body weight ratio (6.04 ± 0.16 mg/g vs. 6.90 ± 0.45 mg/g in untreated TAC mice, $P < 0.01$). These results indicate that amlodipine ameliorates cardiomyocyte hypertrophy via inhibition of EGFR phosphorylation.
© 2004 Elsevier Inc. All rights reserved.

Keywords: Calcium channel blocker; Cardiomyocyte; Hypertrophy; Epidermal growth factor; Phosphorylation; Mouse

Calcium channel blockers (CCBs) are widely used for the treatment of hypertension. Amlodipine is a long-acting dihydropyridine CCB that is effective for lowering the blood pressure, amelioration of cardiac remodeling, and reduction of mortality and morbidity [1]. However, the mechanisms underlying the beneficial effects of CCBs on cardiac remodeling are not fully understood. We have reported that stimulation of the G protein-coupled receptor (GPCR) in cardiomyocytes causes the release of heparin-binding epidermal growth factor (HB-EGF), which subsequently binds to the epidermal growth factor receptor (EGFR) and produces cardiac hypertrophy [2]. There is evidence that calcium channels play an important role in activation of the EGFR [3]. Calcium channels were reported to be involved in endothelin-1-induced activation of the EGFR [3], and calcium channels also induce tyrosine phosphorylation of this receptor to levels that can activate the mitogen-activated protein kinase signaling pathway [4]. In addition, blockade of calcium uptake and mobilization by mammary gland epithelial cells suppress EGF-induced cell proliferation [5]. Considering these findings, we hypothesized that amlodipine may ameliorate cardiomyocyte hypertrophy by inhibiting EGFR phosphorylation. In the present study, we evaluated the effect of amlodipine on EGFR phosphorylation induced by a GPCR agonist in vitro and

* Corresponding author. Fax: +81 6 6836 1120.
E-mail address: kitakaze@zf6.so-net.ne.jp (M. Kitakaze).

0006-291X/$ - see front matter © 2004 Elsevier Inc. All rights reserved.
doi:10.1016/j.bbrc.2004.12.112

on cardiomyocyte hypertrophy induced by left ventricular pressure overload in vivo.

Materials and methods

Cell culture. Rat neonatal ventricular myocytes were isolated as described previously [2], and were cultured in Dulbecco's modified Eagle's medium (DMEM; Sigma) supplemented with 10% FBS (Equitech-Bio). The medium was changed to serum-free medium after 72 h and cells were cultured under serum-free conditions for 48 h before addition of agents. Protein synthesis by the cultured cells was evaluated through analysis of [^{3}H]leucine incorporation [2,6]. Cardiomyocytes were exposed to either epinephrine (Epi: 10^{-5} M) or HB-EGF (10^{-8} M) for 24 h in the presence or absence of amlodipine (kindly provided by Sumitomo Pharmaceuticals, Japan), and the increase of [^{3}H]leucine incorporation was examined.

EGFR phosphorylation. Cultured cardiomyocytes were exposed to 10^{-5} M Epi or 10^{-8} M HB-EGF with or without pretreatment by amlodipine (10^{-6} or 10^{-9} M) or HB-EGF neutralizing antibody #19 for 30 min. Cells were lysed by incubation for 20 min at 4 °C in a buffer (50 mM Tris–HCl, pH 7.3; 150 mM NaCl; 2 mM EDTA; 0.5% sodium fluoride; 10 mM sodium pyrophosphate; 0.5 mM Na_3VO_4; 100 μg/ml phenylmethylsulfonyl fluoride; 2 μg/ml aprotinin; protease inhibitor cocktail; and 1% Nonidet P-40). Immunoprecipitation with an antibody directed against the EGFR and immunoblotting using phosphorylation antibody (Anti-pY) were performed as described elsewhere [7].

Animal model. All procedures were performed in accordance with the institutional guidelines for animal research. Male C57BL/6 mice (8–9 weeks-old, wt 19–25 g) were anesthetized with a mixture of xylazine (5 mg/kg) and ketamine (100 mg/kg intraperitoneally). The animal model of pressure overload was created as described previously [8]. Briefly, transverse aortic constriction (TAC) was produced by tying a 7-0 suture tied twice around the aorta and a 27-gauge needle, after which the needle was gently removed to yield 60–80% constriction of the aortic arch.

To determine whether amlodipine could attenuate cardiac hypertrophy induced by TAC, we treated the mice with saline (TAC group) or oral amlodipine 3 mg/kg/day. To confirm that the extent of pressure overload was similar between the amlodipine-treated and untreated groups, we measured the pressure in the ascending aorta of 2–3 mice from each group using a 1.4 F Millar catheter on the 2nd day after TAC. The tail-cuff blood pressure and heart rate (BP-98A, Softron, Tokyo, Japan) were examined before sacrifice. One week after the induction of pressure overload, mice were killed to determine organ weights and perform morphometric analysis. The cross-sectional surface area of cardiomyocytes was measured using three hearts in each group with the method described previously [6].

Statistical analysis. Multiple comparisons were performed by one-way ANOVA with the Tukey–Kramer exact probability test. Results are reported as means ± SEM. For all analyses, $P < 0.05$ was considered statistically significant.

Results and discussion

Amlodipine attenuates the induction of cardiomyoctyte protein synthesis by epinephrine

As shown in Fig. 1A, amlodipine markedly inhibited epinephrine-induced neonatal rat cardiomyocyte protein synthesis over a concentration range of 10^{-7}–10^{-5} M. Epinephrine is one of the GPCR agonists and is well known to induce cardiomyocyte hypertrophy. Pignier et al. [9] reported that hypertrophy induced by long-term stimulation of α_1-adrenoceptors is accompanied by an increase in the expression of functional calcium channels in neonatal rat cardiomyocytes, indicating the existence of a novel α_1-mediated pathway for positive regulation of the L-type calcium current. This agrees with our finding that blockade of L-type calcium channels inhibits cardiomyocyte hypertrophy. There is substantial evidence to support the notion that calcium signaling pathways contribute to the progression of cardiac hypertrophy [10,11], so it is likely that blockade of calcium signaling would lead to the regression of hypertrophy.

Amlodipine causes concentration-dependent inhibition of EGFR phosphorylation induced by epinephrine

Based on our earlier demonstration that EGFR activation by GPCR agonists led to the development of cardiac hypertrophy [2] and the present in vitro finding that

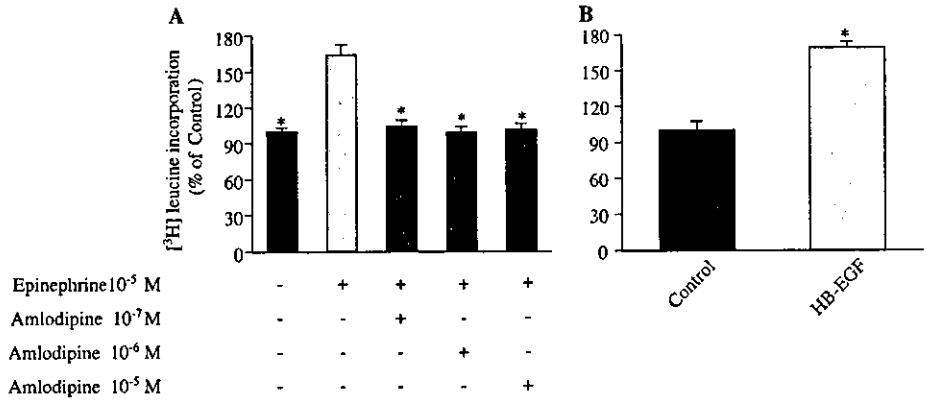

Fig. 1. Effect of amlodipine and HB-EGF on protein synthesis in rat cardiomyocytes. (A) Protein synthesis stimulated by epinephrine (10^{-5} M) was inhibited by amlodipine at concentrations ranging from 10^{-7} to 10^{-5} M. *$P < 0.01$ vs. epinephrine alone. (B) HB-EGF (10^{-8} M) significantly increased myocyte protein synthesis. *$P < 0.01$ vs. Control.

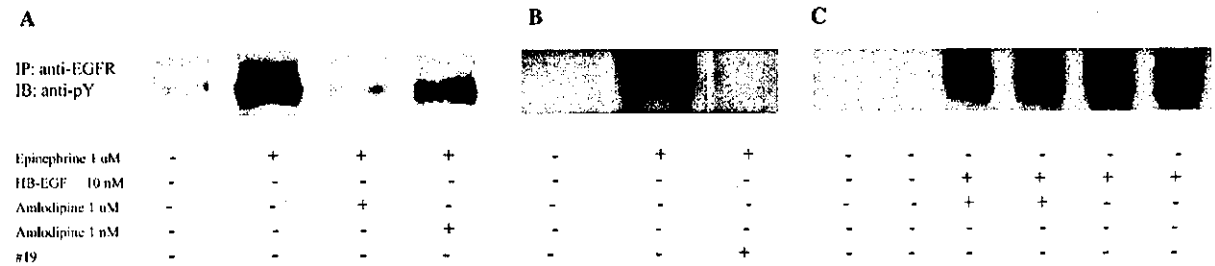

Fig. 2. EGFR phosphorylation and release of HB-EGF. (A) EGFR phosphorylation showed concentration-dependent inhibition by amlodipine. (B) HB-EGF neutralizing antibody #19 blocked epinephrine-induced EGFR phosphorylation. (C) Amlodipine did not influence EGFR phosphorylation induced by HB-EGF. Each experiment was repeated at least three times.

amlodipine inhibits cardiomyocyte protein synthesis stimulated by a GPCR agonist (epinephrine), we hypothesized that amlodipine may also inhibit cardiomyocyte hypertrophy by preventing tyrosine phosphorylation of the EGFR. In the present study, HB-EGF significantly increased protein synthesis by neonatal rat cardiomyocytes (Fig. 1B), a finding that agreed with our previous report [2]. Interestingly, we also demonstrated that amlodipine inhibits EGFR phosphorylation in cardiomyocytes in a concentration-dependent manner (Fig. 2A). In recent years, information about the mechanisms related to Ca^{2+} influx has accumulated. Zwick et al. [12] reported that calcium-dependent EGFR activation led to subsequent activation of the Ras/mitogen-activated protein pathway in neurons. In addition, Kawanabe et al. [3] have shown that Ca^{2+} influx plays an important role in endothelin-1-induced EGFR activation, and endothelin-1 is well known to stimulate cardiomyocyte growth.

Amlodipine inhibits epinephrine-induced release of HB-EGF

We previously reported that phenylephrine induces EGFR activation by increasing the release of the HB-EGF ectodomain [2]. Here we found that amlodipine could inhibit EGFR activation by reducing the epinephrine-induced release of HB-EGF. Since the extracellular level of the ectodomain of HB-EGF (soluble HB-EGF) was generally too low to be detected by Western blotting, we assessed it by an indirect method. If epinephrine induces release of the HB-EGF ectodomain, its depletion was assumed to block epinephrine-induced EGFR activation. As expected, we found that an HB-EGF neutralizing antibody #19 almost completely prevented epinephrine-induced phosphorylation of the EGFR (Fig. 2B), suggesting that epinephrine-induced EGFR activation is mediated by the release of HB-EGF, at least in newborn rat cardiac myocytes. When we investigated whether amlodipine prevents HB-EGF-induced activation of the EGFR, we found that this drug did not have any influence on HB-EGF-mediated EGFR phosphorylation (Fig. 2C), suggesting that it acts upstream of HB-EGF. Finally, we revealed that amlodipine caused marked inhibition of epinephrine-induced phosphorylation of the EGFR (Fig. 2A), a result that supported an inhibitory effect of the drug on EGFR activation by preventing the release of HB-EGF. Further studies are needed to elucidate the exact mechanism by which CCBs inhibit EGFR phosphorylation. Src kinase is reported to contribute to EGFR activation by GPCR agonists [13,14], while a link between calcium release through L-type calcium channels and Src has also been demonstrated [4,15–18], and the release of calcium seems to be necessary for activation of Src [4,18]. Thus, it is likely that amlodipine blocks the signal transduction pathway upstream of Src.

Amlodipine inhibits myocardial hypertrophy in vivo

We used a well-established mouse model of left ventricular pressure overload to further confirm the preventive effect of amlodipine on cardiac hypertrophy. An increase of GPCR agonists, such as catecholamines [6], angiotensin II, and endothelin-1, is known to occur in the myocardium of these mice. Since EGFR activation leads to cardiomyocyte hypertrophy [2] and amlodipine inhibits epinephrine-induced EGFR phosphorylation in cardiomyocytes in vitro, as shown in the present study, it would seem plausible that amlodipine also attenuates cardiac hypertrophy induced by TAC. Indeed, consistent with our in vitro results, we found that oral administration of amlodipine (3 mg/kg/day) for 1 week markedly ameliorated cardiac hypertrophy. Histological examination confirmed that myocyte hypertrophy was less severe (Figs. 3A and B) in mice treated with amlodipine. Compared with sham mice, the heart-to-body weight ratio (HW/BW) increased by about 43% in TAC mice, while the amlodipine-treated mice only showed an increase of about 25% (Fig. 3C). Cardiomyocytes cross-surface area was also significantly decreased in amlodipine-treated mice (Fig. 3D). Hemodynamic parameters are summarized in Table 1; amlodipine did not significantly affect either the tail-cuff systolic blood pressure or the heart rate. Ascending aortic pressure was similar in the TAC and amlodipine-treated TAC

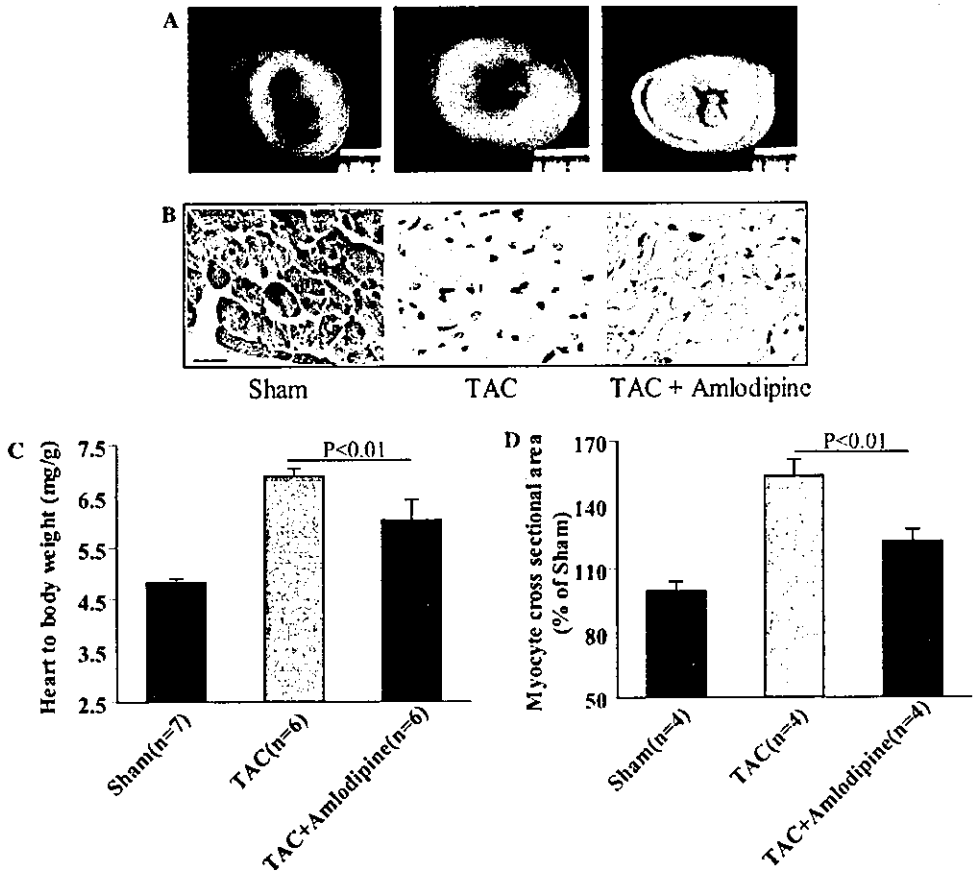

Fig. 3. Effects of amlodipine on cardiac hypertrophy induced by pressure overload in mice. (A) Representative cross-sections of hearts from the three groups. (B) Histological examination showed that cardiomyocyte hypertrophy was less severe in hearts of amlodipine-treated mice (Bar, 20 μm, HE stain). The heart-to-body weight ratio (HW/BW) (C) and cardiomyocyte cross-sectional surface area (D) were significantly lower in TAC mice treated with amlodipine (3 mg/kg/day) in comparison with untreated TAC mice.

Table 1
General characteristics in three experimental groups

Group	AASBP (mmHg)[a]	BW (g)	Tail SBP (mmHg)	HR (bpm)
Sham ($n = 7$)	101 ± 5	23 ± 0.2	112 ± 4	644 ± 26
TAC ($n = 6$)	157 ± 9[b]	22.4 ± 0.3	100 ± 5[b]	670 ± 24
TAC+amlodipine ($n = 6$)	161 ± 8[b]	20.1 ± 0.8[b,c]	93 ± 3[b]	675 ± 19

TAC, transverse aortic constriction; AASBP, ascending aortic systolic blood pressure (SBP); AASBP was measured in three mice in each group at 2nd day after TAC, while those mice were randomly selected and did not receive amlodipine treatment, because we just wanted to confirm that the pressure overload was similar between TAC and amlodipine-treated groups. BW, body weight; HR, heart rate. BW, tail SBP, and HR were measured before sacrifice.

[a] $n = 2$ in each group.
[b] $P < 0.05$ vs. Sham.
[c] $P < 0.05$ vs. TAC.

groups, indicating that there was no significant difference of the pressure load on the left ventricle.

Our data suggested that amlodipine was effective for ameliorating cardiomyocyte hypertrophy independently of any decrease in the blood pressure. This antihypertrophic effect was attributable, at least partly, to the inhibition of EGFR phosphorylation by amlodipine and this drug is also likely to exert an antihypertrophic effect through the nitric oxide signaling pathway, as indicated by previous studies [19].

Although various clinical trials have demonstrated that amlodipine is effective and safe for the treatment of hypertension and reducing cardiac events [20–22], the underlying mechanisms remain poorly understood. The present study is the first to show that amlodipine ameliorates cardiac hypertrophy by inhibiting EGFR

activation. This suggests the possibility of using the regulation of Ca^{2+} influx as a therapeutic approach for controlling cell growth and proliferation.

Acknowledgments

This work was supported by a grant for Research on Sensory and Communication Disorders (H14-tokushitsu-38) from the Health and Labor Sciences Research Grants provided by the Ministry of Health, Labor and Welfare in Japan.

References

[1] J. Muntwyler, F. Follath, Calcium channel blockers in treatment of hypertension, Prog. Cardiovasc. Dis. 44 (2001) 207–216.

[2] M. Asakura, M. Kitakaze, S. Takashima, Y. Liao, F. Ishikura, T. Yoshinaka, H. Ohmoto, K. Node, K. Yoshino, H. Ishiguro, H. Asanuma, S. Sanada, Y. Matsumura, H. Takeda, S. Beppu, M. Tada, M. Hori, S. Higashiyama, Cardiac hypertrophy is inhibited by antagonism of ADAM12 processing of HB-EGF: metalloproteinase inhibitors as a new therapy, Nat. Med. 8 (2002) 35–40.

[3] Y. Kawanabe, N. Hashimoto, T. Masaki, Characterization of Ca^{2+} channels involved in ET-1-induced transactivation of EGF receptors, Am. J. Physiol. Heart Circ. Physiol. 283 (2002) H2671–H2675.

[4] L.B. Rosen, M.E. Greenberg, Stimulation of growth factor receptor signal transduction by activation of voltage-sensitive calcium channels, Proc. Natl. Acad. Sci. USA 93 (1996) 1113–1118.

[5] J. Ichikawa, T. Kiyohara, Suppression of EGF-induced cell proliferation by the blockade of Ca^{2+} mobilization and capacitative Ca^{2+} entry in mouse mammary epithelial cells, Cell Biochem. Funct. 19 (2001) 213–219.

[6] Y. Liao, S. Takashima, Y. Asano, M. Asakura, A. Ogai, Y. Shintani, T. Minamino, H. Asanuma, S. Sanada, J. Kim, H. Ogita, H. Tomoike, M. Hori, M. Kitakaze, Activation of adenosine A1 receptor attenuates cardiac hypertrophy and prevents heart failure in murine left ventricular pressure-overload model, Circ. Res. 93 (2003) 759–766.

[7] S. Tokumaru, S. Higashiyama, T. Endo, T. Nakagawa, J.I. Miyagawa, K. Yamamori, Y. Hanakawa, H. Ohmoto, K. Yoshino, Y. Shirakata, Y. Matsuzawa, K. Hashimoto, N. Taniguchi, Ectodomain shedding of epidermal growth factor receptor ligands is required for keratinocyte migration in cutaneous wound healing, J. Cell Biol. 151 (2000) 209–220.

[8] Y. Liao, F. Ishikura, S. Beppu, M. Asakura, S. Takashima, H. Asanuma, S. Sanada, J. Kim, H. Ogita, T. Kuzuya, K. Node, M. Kitakaze, M. Hori, Echocardiographic assessment of LV hypertrophy and function in aortic-banded mice: necropsy validation, Am. J. Physiol. Heart Circ. Physiol. 282 (2002) H1703–H1708.

[9] C. Pignier, I. Levan-Petit, C. Ancey, D. Potreau, Alpha-adrenoceptor stimulation induces hypertrophy and increases L-type calcium current density in neonatal rat ventricular cardiomyocytes in culture, Receptors Channels 7 (2000) 173–187.

[10] R. Passier, H. Zeng, N. Frey, F.J. Naya, R.L. Nicol, T.A. McKinsey, P. Overbeek, J.A. Richardson, S.R. Grant, E.N. Olson, CaM kinase signaling induces cardiac hypertrophy and activates the MEF2 transcription factor in vivo, J. Clin. Invest. 105 (2000) 1395–1406.

[11] S. Minamisawa, M. Hoshijima, G. Chu, C.A. Ward, K. Frank, Y. Gu, M.E. Martone, Y. Wang, J. Ross Jr., E.G. Kranias, W.R. Giles, K.R. Chien, Chronic phospholamban-sarcoplasmic reticulum calcium ATPase interaction is the critical calcium cycling defect in dilated cardiomyopathy, Cell 99 (1999) 313–322.

[12] E. Zwick, H. Daub, N. Aoki, Y. Yamaguchi-Aoki, I. Tinhofer, K. Maly, A. Ullrich, Critical role of calcium-dependent epidermal growth factor receptor transactivation in PC12 cell membrane depolarization and bradykinin signaling, J. Biol. Chem. 272 (1997) 24767–24770.

[13] B.H. Shah, M.P. Farshori, A. Jambusaria, K.J. Catt, Roles of Src and epidermal growth factor receptor transactivation in transient and sustained ERK1/2 responses to gonadotropin-releasing hormone receptor activation, J. Biol. Chem. 278 (2003) 19118–19126.

[14] Q. Zhang, S.M. Thomas, S. Xi, T.E. Smithgall, J.M. Siegfried, J. Kamens, W.E. Gooding, J.R. Grandis, SRC family kinases mediate epidermal growth factor receptor ligand cleavage, proliferation, and invasion of head and neck cancer cells, Cancer Res. 64 (2004) 6166–6173.

[15] H. Schottelndreier, B.V. Potter, G.W. Mayr, A.H. Guse, Mechanisms involved in alpha6beta1-integrin-mediated Ca(2+) signalling, Cell. Signal. 13 (2001) 895–899.

[16] K.R. Waitkus-Edwards, L.A. Martinez-Lemus, X. Wu, J.P. Trzeciakowski, M.J. Davis, G.E. Davis, G.A. Meininger, alpha(4)beta(1) Integrin activation of L-type calcium channels in vascular smooth muscle causes arteriole vasoconstriction, Circ. Res. 90 (2002) 473–480.

[17] X. Wu, G.E. Davis, G.A. Meininger, E. Wilson, M.J. Davis, Regulation of the L-type calcium channel by alpha 5beta 1 integrin requires signaling between focal adhesion proteins, J. Biol. Chem. 276 (2001) 30285–30292.

[18] Y. Zou, A. Yao, W. Zhu, S. Kudoh, Y. Hiroi, M. Shimoyama, H. Uozumi, O. Kohmoto, T. Takahashi, F. Shibasaki, R. Nagai, Y. Yazaki, I. Komuro, Isoproterenol activates extracellular signal-regulated protein kinases in cardiomyocytes through calcineurin, Circulation 104 (2001) 102–108.

[19] S. Sanada, K. Node, T. Minamino, S. Takashima, A. Ogai, H. Asanuma, H. Ogita, Y. Liao, M. Asakura, J. Kim, M. Hori, M. Kitakaze, Long-acting Ca^{2+} blockers prevent myocardial remodeling induced by chronic NO inhibition in rats, Hypertension 41 (2003) 963–967.

[20] M. Packer, C.M. O'Connor, J.K. Ghali, M.L. Pressler, P.E. Carson, R.N. Belkin, A.B. Miller, G.W. Neuberg, D. Frid, J.H. Wertheimer, A.B. Cropp, D.L. DeMets, Effect of amlodipine on morbidity and mortality in severe chronic heart failure. Prospective Randomized Amlodipine Survival Evaluation Study Group, N. Engl. J. Med. 335 (1996) 1107–1114.

[21] R.A. Kloner, M. Weinberger, J.L. Pool, S.G. Chrysant, R. Prasad, S.M. Harris, T.M. Zyczynski, N.K. Leidy, E.L. Michelson, Comparative effects of candesartan cilexetil and amlodipine in patients with mild systemic hypertension. Comparison of candesartan and amlodipine for safety, tolerability and efficacy (CASTLE) study investigators, Am. J. Cardiol. 87 (2001) 727–731.

[22] ALLHAT Officers and Coordinators for the ALLHAT Collaborative Research Group. Major outcomes in high-risk hypertensive patients randomized to angiotensin-converting enzyme inhibitor or calcium channel blocker vs diuretic: The Antihypertensive and Lipid-Lowering Treatment to Prevent Heart Attack Trial (ALLHAT), JAMA 288 (2002) 2981-2997.